Under the cover of darkness: a transcriptomic exploration of clubroot during the night.

Andrea Garvetto[1], Susann Auer[2], Freia Benade[2], Michaela Hittorf[1,3], Jutta Ludwig-Müller[2], Sigrid Neuhauser[1]

Corresponding authors: Andrea Garvetto (andrea.garvetto@uibk.ac.at), Sigrid Neuhauser (sigrid.neuhauser@uibk.ac.at)
[1]Department of Microbiology, Universität Innsbruck, Technikerstraße 25, 6020 Innsbruck, Tirol, Austria.
[2]Faculty of Biology, Technische Universität Dresden, 01062 Dresden, Germany.
[3]Department of Botany, Universität Innsbruck, Sternwartestraße 15, 6020 Innsbruck, Tirol, Austria.

Summary

Plasmodiophora brassicae (Phytomyxea, Rhizaria) is the etiological agent of clubroot disease, one of the most important diseases of Brassicaceae crops. Alteration of metabolism and hormone homeostasis leads to the formation of tumour-like galls in the roots of affected plants. Host plant energy metabolism, defence and developmental processes are under strong temporal control and the very same processes are affected by clubroot. For the first time, this study uses time-resolved transcriptome analyses to explore how *P. brassicae* affects *Arabidopsis thaliana* in the night during intermediate (14 days after inoculation; DAI) and late (21 DAI) infection. Day-night differences in gene expression were more pronounced in younger rather than older plants in our differential gene expression (DGE) analysis. Consequently, intermediate phases of infection showed more day-night differences than later ones. Clustering of differentially expressed genes (DEGs) in functional categories highlighted how some of the typical processes known to be disrupted by clubroot infection are more significantly affected in the night and also uncovered some disrupted exclusively in the night. RNA modification stood out as the most unambiguously upregulated process in infected *Arabidopsis* roots in the night. Analysis of the interaction between clubroot infection and diel oscillations in gene expression detected modifications in the rhythmicity of central circadian clock components during the infection. We discuss our findings in the context of manipulation of plant defence and metabolism, identifying targets for experimental validation and highlighting potential new lines of investigation of our time-resolved datasets to better understand the interaction between *P. brassicae* and its host.

Significance statement: *Plasmodiophora brassicae* impacts physiological processes under strong temporal control in Brassicaceae hosts: e.g., metabolism, hormone homeostasis and defence. Here, for the first time, we performed a time-resolved transcriptomic exploration of clubroot disease at intermediate and mature stages of infection. We identify a previously unrecognised role for nocturnal manipulation of organellar RNA editing and disruption of rhythmicity in circadian clock components. We provide a dataset enabling further exploration of the impact of clubroot on plant circadian processes.

Keywords: Biotrophic parasite, Circadian, Host-pathogen interactions, *Plasmodiophora brassicae,* Protist, Time-resolved transcriptome, *Arabidopsis thaliana*.

Introduction

Responsible for around 10 % of harvest losses worldwide, *Plasmodiophora brassicae* Woronin is one of the most impactful pathogens of Brassicaceae crops (Dixon, 2009). This obligate biotrophic parasitic protist belonging to the class Phytomyxea (Rhizaria; Sierra et al., 2016) has a complex life cycle featuring a short-lasting, symptomless primary phase occurring in the root hairs and epidermis of a broad array of plant hosts; and a secondary, long-lasting and symptomatic phase, specifically occurring in hosts within the family Brassicaceae where durable resting spores are formed (Kageyama & Asano, 2009; Liu et al., 2020). The secondary phase of the infection occurs in the root cortex and stele, where it impacts the host physiology and anatomy, causing successive hyperplasia and hypertrophy in the affected tissues (Olszak et al., 2019), leading to the typical gall formation from which the common name "clubroot disease" derives. This modification of the host anatomy and physiology is required for the parasite to generate a strong local nutrient sink at the site of infection, inducing a systemic redirection of the host photosynthates (Malinowski et al., 2019). Clubroot impact on susceptible plants is heavy, with infected hosts featuring stunted growth, increased susceptibility to wilting and early onset of senescence (Javed et al., 2023). Molecular investigations have been proven paramount in understanding the influence of *P. brassicae* on its host physiology (Agarwal et al., 2011; Ciaghi et al., 2019; Irani et al., 2018; Siemens et al., 2006), highlighting highly impacted processes deserving more extensive investigation, such as: cell wall expansion, remodelling and lignification (Stefanowicz et al., 2021; Tu et al., 2024); cell cycle activation and modification (Olszak et al., 2019) and sugar homeostasis (Siemens et al., 2011). Pathogen-induced disruption of sugar homeostasis is crucial to the trophic interaction between *P. brassicae* and its host, whereby the parasite generates a sugar sink in the gall tissue by increasing symplastic sugar delivery via extracellular invertases (Siemens et al., 2011) and by promoting phloem differentiation and local accumulation of sugar transporters at the site of infection (Walerowski et al., 2018).

62 Because of its central role in plant physiology, the disruption of sugar metabolism likely mediates
63 systemic reactions at the organism level in clubroot disease, but the substantial anatomical changes
64 observed are also the result of its impact on hormone homeostasis (Devos et al., 2006; Ludwig-Müller et
65 al., 2009). Hormones involved in plant defence such as salicylic acid (SA) and jasmonic acid (JA) have
66 been broadly linked to heightened resistance against *P. brassicae* (Gravot et al., 2012; Lemarié et al.,
67 2015; Lovelock et al., 2013, 2016); and the parasite seems to directly disrupt both (Ludwig-Müller et al.,
68 2015; Smolko et al., 2024). *P. brassicae* also induces accumulation of the stress-related hormone abscisic
69 acid (ABA) as a consequence of the impaired vascular transport and water supply caused by gall
70 formation (Ludwig-Müller et al., 2009). *Arabidopsis* mutants impaired in the perception of the stress-
71 related hormone ethylene (ET) showed increased resistance only when the mutation targeted the
72 crosstalk between ethylene and auxin transport (Ludwig-Müller et al., 2009; Vandenbussche et al.,
73 2003). Indeed, auxins have been found to play an important role in clubroot disease, gradually increasing
74 in the galls with the development of the infection and mutants impaired in indole acetic acid (IAA)
75 biosynthesis were found to produce smaller or developmentally delayed galls (Grsic-Rausch et al., 2000;
76 Neuhaus et al., 2000). Investigations highlighted how the *P. brassicae* protein PbGH3 can conjugate
77 auxins (Smolko et al., 2024) and the recently identified gene *SYNERGISTIC ON AUXIN AND CYTOKININ 1*
78 (*SYAC1*), a cross-talk component between the auxin and cytokinin pathways in *A. thaliana* roots, made
79 plants more susceptible to infection and exacerbated the symptoms of clubroot when constitutively
80 expressed; supporting a pivotal role of the auxin-cytokinin balance in this interaction (Hurný et al., 2020).
81 In biotrophic interactions between plants and pathogens, the role of cytokinins in establishing local
82 nutrient sinks and in suppressing cell death has long been recognized (Walters & McRoberts, 2006),
83 nonetheless the overall impact of *P. brassicae* on host cytokinins is ambiguous. Studies have reported
84 both suppression and increase in metabolism and levels of cytokinins (Dekhuijzen, 1981; Dekhuijzen &
85 Overeem, 1971; Malinowski et al., 2016), but decreased cytokinin degradation on the host side (Siemens
86 et al., 2006) coupled with evidence of endogenous cytokinin production by the pathogen (Müller &

87 Hilgenberg, 1986; Rolfe et al., 2016) seem to support the need for cytokinins in the local establishment
88 of a *de novo* meristematic sink area in the initial phases of infection (Devos et al., 2005, 2006).

89 The above listed processes impacted by *P. brassicae* are known to be strongly influenced by diel (i.e., day
90 and night) and circadian oscillations in plants. While most living organisms have evolved a way to
91 synchronise their physiology to the environmental rhythms in order to maximize their fitness, plants are
92 particularly affected by these rhythms as they rely for growth and development on light, arguably one of
93 the most rhythmic timers/*zeitgebers* on the planet (Henriques et al., 2018; Sanchez & Kay, 2016).
94 Changes in light and other oscillating environmental parameters such as temperature, entrain the core
95 circadian clock, a transcriptional/translational feedback loop central to the adjustment of rhythmic
96 physiological responses in plants (S. Wang et al., 2022). Moreover, the same rhythmic physiological
97 processes influenced by environmental factors via the circadian clock also act back on it as endogenous
98 *zeitgebers* such as in the case of sugars derived from photosynthetic carbon fixation, whose correlation
99 with the availability of diurnal light has long been ascertained (Graf et al., 2010; Mora-García et al.,
100 2017).

101 Besides being under strong temporal control, the availability of photosynthates is also spatially resolved.
102 For example, a sucrose transporter involved in phloem unloading has been found to be specifically
103 upregulated in roots during the night, matching a steady increase in nocturnal root growth that peaks
104 shortly after dawn (Durand et al., 2018; Yazdanbakhsh et al., 2011; Yazdanbakhsh & Fisahn, 2010). The
105 synthesis and accumulation of defence hormones has also been reported to be under the influence of
106 diel oscillations in gene expression, in particular the synthesis and accumulation of competing JA and SA;
107 with JA-mediated resistance to herbivores and necrotrophic pathogens being upregulated in the day,
108 whilst SA-mediated resistance to biotrophic parasites heightened in the night (Goodspeed et al., 2012).
109 As already mentioned, the majority of the processes under circadian control also provide retroactive
110 feedback to inform and entrain the circadian clock itself (S. Wang et al., 2022). Since pathogens are

known to manipulate hormones and to strongly affect energy homeostasis, it is possible that these processes are central to mediate pathogen-induced modifications on the host internal clock (Lu et al., 2017).

Many biotrophic parasites have been shown to possess intrinsic transcriptionally-mediated rhythms (Rijo-Ferreira et al., 2017, 2020) and in well-investigated pathosystems, such as *Plasmodium* spp. in vertebrates, the parasite contemporarily synchronizes with (Motta et al., 2023) and disrupts (Prior et al., 2019) the circadian rhythmicity of the host.

We reasoned that, as an obligate biotrophic intracellular parasite, *P. brassicae* is likely to have evolved similar ways to influence the rhythmic gene expression of its host in order to maximize its benefits and hinder defence; especially considering its strong influence on host diel processes such as for example carbohydrates allocation to the root (Graf et al., 2010; Malinowski et al., 2019; Yazdanbakhsh et al., 2011). Nevertheless, until now only the diurnal phase of clubroot infection has been explored. This study aims at providing the first time-resolved RNA-seq dataset, covering both day and night, for intermediate (14 days post-inoculation) and mature (21 days post-inoculation) clubroot disease in *Arabidopsis thaliana.* We provide a first exploration of the data generated in order to highlight processes of the host that are influenced by the parasite specifically during the night and further to understand the interplay between diurnal/nocturnal changes in gene expression and clubroot disease.

Results

Overview of gene expression levels in infected and healthy plants in the day and in the night

The major factor influencing the clustering of DEGs of *A. thaliana* in PCAs is their response to *P. brassicae* (Fig. 1 A & C). In the intermediate phases of infection (14 DAI) the first two principal components (PCs) explain a cumulative 78% of the variation (Fig. 1 A). Infected and healthy plants strongly separate along the PC1, explaining more than half of the variation in gene expression (63%). Noticeably, the PC2

134 (explaining 15% of the variation) mostly separated the samples according to night or day (factor "Time
135 point"). Samples collected at 21 DAI seem to be less affected by the time of sampling, with PC1
136 explaining 83% of the variation and being clearly linked to the infected or healthy status of the plant
137 samples, and PC2 explaining only 5% of the variation (Fig. 1 C) without clear separation of the samples
138 along the factor "Time point". A PCA of the gene expression levels in uninfected plants resulted in a
139 similar pattern, whereby older plants did not show a time-dependent response (Additional File 3).
140 Befittingly, in plants 14 DAI more than one third (36,75%) of the differentially expressed genes (DEGs)
141 are specific to the night phase and 16,40% to the day (Fig. 1 B), whilst the proportion of DEGs that are
142 exclusively detected during day or night is decreasing at 21 DAI indicating a reduced influence of the
143 factor "Time point" on gene expression from the intermediate to the late stages of infection (21,48% in
144 the night, 17,52% in the day and 61% shared; Fig. 1 D).

145 *Regulation of enriched GO categories in infected plants during day and night*

146 Differentially expressed genes (DEGs) were largely downregulated in infected plants across all sampling
147 times and DAI, as shown in Additional Files 4 and 5. This overall trend was further confirmed through an
148 analysis of average expression levels within overrepresented Gene Ontology (GO) categories, which
149 revealed a consistent predominance of downregulated over upregulated categories.

150 At 14 DAI during the day, this imbalance was particularly evident: 63 GO categories showed
151 downregulation compared to just 25 that were upregulated, while one category— "response to molecule
152 of fungal origin"—exhibited an equal mix of both (Fig. 2A and Additional File 6).

153 The ten most significantly upregulated categories during the day were associated with responses to
154 environmental stress, development, and biosynthesis, with highly significant enrichment seen in
155 processes such as response to toxic substances, anatomical structure morphogenesis, pigment
156 biosynthesis, and photosynthetic activity. In contrast, the most significantly downregulated categories

157 were related to core metabolic and defense responses, including hypoxia response, carbohydrate
158 metabolism, salicylic acid signaling, and floral development (Fig. 2 A and Additional File 6).

159 A similar expression pattern was observed during the night at 14 DAI, with 67 GO categories
160 downregulated and 30 upregulated, alongside five showing no overall change (Fig. 2B and Additional File
161 6). Upregulated categories at night included many processes related to stress-response and signaling
162 such as response to toxic substance, RNA modification, ABC-type transporter activity, and response to
163 reactive oxygen species. Meanwhile, downregulated categories again pointed to a suppression of key
164 metabolic and defense functions, including phenylpropanoid metabolism, oxygen response, glycoside
165 metabolism, and response to salicylic acid.

166 By 21 DAI, the contrast between down- and upregulated categories became even more pronounced,
167 consistent with the higher number of DEGs observed at this later stage of infection (Fig. 3, Additional
168 Files 5 and 9). During the day, 94 categories were downregulated compared to just 15 upregulated.
169 These upregulated categories continued to reflect photosynthetic and light-responsive processes, such
170 as plastid organization, pigment biosynthesis, circadian rhythm regulation, and peroxisomal activity.
171 Conversely, the most downregulated categories included pathways related to toxic substance response,
172 carbohydrate metabolism, extracellular signaling, and salicylic acid response, indicating a persistent
173 suppression of metabolic and defense processes.

174 At night, the upregulated GO categories again included several also enriched during the day, such as
175 photosynthesis and plastid organization. Additional night-specific upregulated processes included
176 responses to light intensity, chlorophyll biosynthesis, and abiotic stress. Downregulated categories at
177 night often mirrored those observed during the day, particularly in areas such as carbohydrate
178 metabolism, tetrapyrrole binding, and external encapsulating structure organization. However, some
179 processes—such as inorganic ion transport and secondary metabolite biosynthesis—were uniquely or
180 more strongly suppressed during the night phase.

181 All GO terms and their associated gene lists used prior to plotting in Figures 2 and 3 are provided in
182 tabular format in Additional File 10.

183 *Effect of the interaction between clubroot and time of the day on A. thaliana gene expression*

184 The variables "Condition" and "Time Point" are not fully independent, both influence gene expression at
185 the same time. To identify the genes that are affected by both of these variables we used a statistical
186 "interaction effect" model (IE; Duda et al., 2023). This identified 217 functionally annotated genes at 14
187 DAI which were strongly impacted by both variables (Fig. 4). These 217 DEGs can be grouped in eight
188 clusters according to their expression patterns. Enriched GO terms could be detected in 6 of these
189 clusters (cluster 1, 3, 4, 5, 6 and 8) hinting at how infection and time of the day are affecting processes in
190 the host (Additional File 8 GO terms overrepresentation analysis of clusters of DEGs driven by the
191 interaction between infection and time of the day 14 DAI8).

192 Clusters 1 and 3 are characterised by a loss of diel oscillation in infected plants, where the genes are
193 always active regardless of the time of the day. Cluster 1 is enriched in the terms related to senescence,
194 circadian rhythm and cell signalling, where control plants show upregulation during the day. Cluster 3 is
195 characterised by the terms “response to nitrate” (particularly enriched in genes encoding glutaredoxins
196 or GRXS; Ehrary et al., 2020) and terms related to the chloroplast membrane (enriched in genes encoding
197 chlorophyllide a oxygenase, chloro-ribosomal subunits and FKBP16-2), terms showing upregulation in the
198 night in the control. Cluster 7 also loses diel oscillation, but the changes in this cluster are characterised
199 by a downregulation of genes in infected plants which are upregulated during day in control plants.

200 In contrast cluster 2 acquires a diel oscillation in infected plants with genes being upregulated in the day
201 and downregulated in the night, an oscillation absent in the control plants. Genes in cluster 6 show an
202 inversion of the normal pattern of expression, whereby nocturnal upregulation in the control is
203 overridden in infected plants by a nocturnal downregulation (and vice versa). Cluster 6 is enriched in

term “response to fructose”. Cluster 4, enriched in terms related to glycosylation of proteins, shows upregulation by the infection with a stronger effect during the day. Clusters 5 and 8 show no distinct pattern. Cluster 5 is associated with the terms “phosphatidylinositol phosphate kinase activity”, “phosphotransferase activity, phosphate group as acceptor” and “nucleoside transmembrane transporter activity” and cluster 8 with terms related to cellular response to abiotic stress and protein localization to the nucleus.

Fewer genes were impacted by the interaction between time of day and infection at 21 days post-infection (DAI) compared to 14 DAI (96 genes with functional annotations). The clustering of the samples cannot discriminate day and night but it maintains a clear separation along infected and control plants (Fig. 5). The pattern of gene expression could divide the DEGs in five clusters, three of which contain enriched GO terms (Additional File 9). Genes in cluster 1 and cluster 2 show a general upregulation in infected plants and in cluster 2 terms related to response to hypoxia and sugars were enriched. Cluster 3 shows an opposite pattern, with genes mainly downregulated by the infection enriching categories related to the development of anatomical structures and cytoplasmic stress granules. The main expression pattern identified in cluster 4 is the upregulation of genes normally downregulated during the night. This cluster is described by GO terms related to circadian/rhythmic processes, chloroplast membranes, histone methylation and transport of organic acids. Cluster 5 shows a more complex expression pattern, were most of the genes upregulated in the night in control conditions are upregulated in the night in infected conditions and vice versa, but no enriched GO terms were found for this cluster.

Discussion

This study explores the effects of *P. brassicae* infection on transcriptional diel oscillations in *A. thaliana*, identifying significant effects on gene expression dynamics. Intermediate infection stages (14 DAI) show strong diel influence, aligning with peak metabolic activity of the parasite and initiation of gall formation

228 (Devos et al., 2005; Liu et al., 2020), whereas later stages (21 DAI) reveal reduced rhythmicity, likely
229 driven by plant senescence rather than the pathogen. Nonetheless, overall the strongest driver of gene
230 expression changes is the infection itself, overriding time-of-day effects, and highlighting a complex
231 interaction between host circadian mechanisms and pathogen strategies. Processes such as
232 phenylpropanoid metabolism and RNA modification are disproportionately affected at night and we link
233 these to disruptions of organellar dynamics and defense in infected roots.

234 Time-resolved RNA-seq analysis of clubroot disease in *A. thaliana* shows an increasing number of DEGs
235 as the infection advances, reflecting the progressive cell-by-cell colonisation of roots by *P. brassicae*
236 (Kunkel, 1918) and its systemic and diversified impact on the plant, where each cell in infected tissues
237 may contain parasitic plasmodia at different stages of development. Existing transcriptomic datasets
238 featuring a developmental dimension support this (Irani et al., 2018; Schuller et al., 2014). The effect of
239 diel changes in gene expression in infected plants appear to be stronger at 14 DAI as compared to 21 DAI
240 (Fig.1) and a decreased influence of day and night on gene expression is also evident in control plants
241 (Additional File 3) indicating a general circadian dampening with plant age. The relationship between
242 senescence and circadian rhythm in ageing plants has been studied in leaves, revealing a similar pattern
243 of reduced amplitude and an increase in frequency of circadian oscillations with age (Kim & Hong, 2019;
244 Lee et al., 2021; Song et al., 2018). A specific circadian clock or 'root clock' has been shown to integrate
245 exogenous cues such as light, water availability and temperature in order to adjust root gene oscillations
246 with the external environment (Bustillo-Avendaño et al., 2022). The root clock is closely linked to shoot
247 apical meristem circadian oscillations (Davis et al., 2022; Mortada et al., 2024; Perez-Garcia et al., 2022)
248 and likely influenced by senescence in above ground tissues, although specific work on the root
249 developmental clock has not yet addressed its interplay with root senescence itself (Siqueira et al.,
250 2022). At 21 DAI clubroot infected *A. thaliana* plants are four weeks old and therefore approaching the
251 end of their six-week life-cycle (Meinke et al., 1998). This advanced senescence would explain the

252 reduced influence of diel rhythmicity observed at 21 DAI (Fig. 1 C&D, 3 and 5). In contrast, a clear
253 influence of night and day has been observed at 14 DAI (14 DAI; Fig. 1 A&B, 2 and 4).

254 The infection is the strongest driver of changes in gene expression (Fig. 1 A), but the genes affected differ
255 between day and night especially in the intermediate phases (i.e., 14 DAI; Fig. 2 and 3; Additional Files 6
256 and 7). GO categories enriched by infection-related DEGs during the day are in line with previous,
257 comparable studies (Ciaghi et al., 2019; Irani et al., 2018). Nonetheless, interpreting these results
258 requires careful consideration, since each enriched GO category contains upregulated and
259 downregulated genes and since the z-score reflects only the count of genes up/downregulated but not
260 the magnitude of changes. For example, specific genes involved in low oxygen responses during clubroot
261 such as PYRUVATE DECARBOXYLASE 1 (PDC1) and ALCOHOL DEHYDROGENASE 1 (ADH1) have been
262 found to be upregulated in previous studies (Gravot et al., 2016). These specific genes are also
263 upregulated in our dataset, even though low oxygen response categories are overall downregulated (Fig.
264 2). Similarly, cell wall-related categories are consistently downregulated in our dataset, though individual
265 genes like expansins and pectin methylesterases show contrasting gene-specific expression patterns,
266 which is in line with previous findings (Ciaghi et al., 2019; Irani et al., 2018; Stefanowicz et al., 2021).

267 The GO term "RNA modification" was the most striking night-exclusive category in terms of differential
268 expression, gene counts and significance at 14 DAI. The majority of genes (90/101) are assigned to
269 pentatricopeptide repeat-containing proteins (PPR proteins), with most of them being upregulated
270 (86/101) and part of the PLS-class PPR proteins (67/101). Land plant genomes harbour an expanded
271 number of PPR protein encoding genes, specifically PLS (Barkan & Small, 2014), and many of them are
272 involved in the RNA stabilisation, splicing and editing in chloroplasts and mitochondria, necessary for the
273 correct development and functioning of the target organelle (Barkan & Small, 2014; X. Wang et al.,
274 2021). These data thus suggest a pivotal role for nocturnal manipulation of mitochondria and plastids by
275 *P. brassicae.*

276 On the one hand, the upregulation of genes potentially involved in organelle dynamics in infected *A.*
277 *thaliana* would fit the well-documented phenomenon of accumulation of amyloplasts in the root cortex
278 of plants affected by clubroot (Garvetto et al., 2023; Ma et al., 2022). Disruption of transcription is
279 known to inhibit the differentiation of plastids into amyloplasts (Enami et al., 2011; Liebers et al., 2017),
280 suggesting a potential involvement of post-transcriptional editing in the transition. Furthermore,
281 cytokinin concentration, another factor necessary for the transition to amyloplast (Enami et al., 2011), is
282 increased locally by *P. brassicae* (Müller & Hilgenberg, 1986; Siemens et al., 2006) arguing for its
283 importance in clubroot development. Amyloplast induction driven by alterations in the cytokinins-to-
284 auxins ratio would enable the storage of sugars directed toward the rapidly growing root in the night
285 (Graf et al., 2010; Yazdanbakhsh et al., 2011; Yazdanbakhsh & Fisahn, 2010), where the parasite
286 generates an even stronger physiological sink (Keen & Williams, 1969; Malinowski et al., 2019;
287 Walerowski et al., 2018). Nevertheless, on the other hand, plastidial RNA editing has been found to be
288 more effective in green tissues as compared to non-photosynthetic ones (Peeters & Hanson, 2002) and a
289 high proportion of PPR in our data seem to target the mitochondrion. Therefore, a hypothesis
290 encompassing organelle-mediated defences might be more parsimonious.

291 RNA editing is required for the correct functioning of chloroplasts and mitochondria and mutations of
292 PPR proteins often lead to defective growth or lethal phenotypes, in particular by stimulating the
293 production of reactive oxygen species (ROS) due to defects in the post-transcriptional modifications of
294 genes targeting these two organelles (Y. Wang & Tan, 2025). Evidence exists of plants exploiting
295 increased ROS levels caused by the disruption of the electron transport chain in chloroplasts and
296 mitochondria as a signal to promote defence or to initiate oxidative burst and fend off pathogens. In *A.*
297 *thaliana* chloroplasts, reduced editing of *ndhB* mRNA (encoding the B subunit of the chloroplast NADH
298 dehydrogenase-like complex - NDH) caused by the disruption of PPR proteins CRR21 and CRR2 (both
299 upregulated in our dataset) led to substantially enhanced ROS production and subsequent resistance to

300 fungal pathogens (García-Andrade et al., 2013). A recent study found that lack of editing and splicing of
301 mitochondria-targeting mRNAs *nad1*, *nad3*, *nad6* and *nad7* (encoding subunits of mitochondrial Complex
302 I) caused by downregulation of the PPR protein RESISTANCE TO PHYTOPHTHORA PARASITICA 7 (RTP7)
303 results in ROS overproduction, oxidative burst and incompatible interaction with the pathogenic
304 oomycete *Phytophthora parasitica*(Yang et al., 2022) Although not a PPR, multiple organellar RNA-
305 editing factor 8 (MORF8) participates in RNA editing in both chloroplasts and mitochondria, and has been
306 shown to decrease resistance to *P. parasitica* when targeting the mitochondrion, putatively by stabilizing
307 the respiratory chain thereby avoiding ROS production, SA signalling and oxidative burst (Yang et al.,
308 2020). This is particularly interesting as *morf8* is among the genes assigned to "RNA modification"
309 upregulated in the night in our analysis. Therefore, the increased RNA editing observed in our dataset
310 can be interpreted as an attempt from the side of *P. brassicae* to maintain functional mitochondria and
311 plastids, subsequently dampening ROS production and defence. The hormone salicylic acid (SA)
312 stimulates mitochondrial ROS production (J. Wang et al., 2022) and is involved in a positive feedback
313 loop (Mencia et al., 2020), suppressing mitochondrial RNA editing and being induced by the ensuing ROS
314 production as observed in (Yang et al., 2020). SA is also under strong diel control and peaks in the middle
315 of the night (Zheng et al., 2015; Lu et al., 2017; Karapetyan & Dong, 2018), therefore disruptions in SA
316 signalling by *P. brassicae* in the moment of its normal peak concentration might help to explain the
317 enhanced nocturnal upregulation of "RNA modification" in our analyses.

318 Indeed, SA-mediated defences are known to be affected in the interaction between *P. brassicae* and its
319 host (Galindo-González et al., 2020; Mencia et al., 2022), as exemplified by the parasite's effector protein
320 PbBSMT methylating SA to methyl-salicylate (MeSA) in order to enhance its transport away from the site
321 of infection, thereby reducing its local concentration and dampening the immune response (Djavaheri et
322 al., 2019; Ludwig-Müller et al., 2015). Accordingly, an overall downregulation of the category "response

323 to salicylic acid" was observed in our analyses in the intermediate and mature infection regardless of the
324 time of the day (Fig. 2 and 3; Additional File 10).

325 A putative targeting of nocturnal SA signalling by *P. brassicae* might also explain why the biosynthesis of
326 phenylpropanoids, enhanced by SA (J. Y. Chen et al., 2006), is more severely impacted in the night (64
327 genes enriching the category "phenylpropanoid metabolic process" in the night as compared to 49 in the
328 day; Additional File 10; Bauters et al., 2021). Phenylpropanoids are known to be involved in plant
329 mechanical and chemical defence, especially via the induction of lignin deposition in secondary cell walls
330 and the accumulation of flavonoids (Dong & Lin, 2021). The pivotal importance of lignification of
331 secondary cell walls in preventing the colonization and spread of *P. brassicae* is known, with the parasite
332 actively interfering in this process in susceptible *B. napus* varieties (Tu et al., 2024) and downregulation
333 of lignin biosynthesis has been observed in clubroot infected *A. thaliana* (Agarwal et al., 2011). Our data
334 suggest that the manipulation of the nocturnally gated SA response by *P. brassicae* is a key driver of the
335 changes observed in defence and organellar dynamics, arguing in favour of the exploration of nocturnal
336 phases of clubroot to better understand this disease. Furthermore, the recently established link between
337 SA acid and circadian clock(Fraser et al., 2024) advocates for the identification of genes whose
338 oscillations are equally affected by temporal and disease dynamics.

339 The IE model allowed for the detection of this small and interesting subset of DEGs whose expression
340 pattern is simultaneously affected by time of the day and infection (Duda et al., 2023). The overall
341 reduction of DEGs at 21 DAI as compared to 14 DAI (i.e., 96 against 217) is likely due to the already
342 observed decreased effect of diel oscillations in older plants and explains the absence of day/night
343 grouping of the samples at 21 DAI (Fig. 5). At 14 DAI, when the effect of time on gene expression is
344 stronger, DEGs appropriately divide samples into day/night and infected/control groups (Fig. 4). At 14
345 DAI, row clustering reveals varying effects of infection on the diel gene expression patterns, the most
346 notable being the suppression of rhythmicity through upregulation of genes that are normally

347 downregulated at night (i.e., cluster 1 in Fig. 4). Interestingly, the GO term enrichment analysis of the
348 DEGs in cluster 1 features the terms “Circadian rhythm” and “Rhythmic process” (Additional File 8). A
349 closer look at the list of genes contained in cluster 1 revealed seven genes of acknowledged importance
350 in rhythmic and circadian processes: *GIGANTEA* (GI), *PSEUDO-RESPONSE REGULATOR* 3 (PRR3), 7 (PRR7)
351 and 9 (PRR9); *PHYTOCHROME INTERACTING FACTOR 4* (PIF4), *NIGHT LIGHT-INDUCIBLE AND CLOCK-*
352 *REGULATED* 1 (LNK1) and 4 (LNK4). Members of the core circadian clock such as GI and the PRRs are
353 known to be directly involved in the transcriptional/translational feedback loop central to circadian
354 oscillations (Sanchez & Kay, 2016), but also to integrate endogenous and exogenous stimuli to inform
355 and entrain it (S. Wang et al., 2022), a role they share with PIF4 and LNK1/4 (Kidokoro et al., 2023; Zhu et
356 al., 2016). Whilst LNK1 and LNK4 seems to mainly integrate temperature stimuli in the circadian
357 oscillator (Kidokoro et al., 2023), all other genes detected above are variously involved in the integration
358 of information about temperature, light, sugar and hormone levels within the circadian clock (S. Wang et
359 al., 2022). While temperature and light are unlikely to be involved in mediating the pathogen influence
360 on the diel rhythm of the host, *P. brassicae* influence on hormones (Jayasinghege et al., 2023; Wei et al.,
361 2021) and sugar levels (Keen & Williams, 1969; Ma et al., 2022) is documented and a more plausible
362 mediator. Considering the suppression of the diel cycle observed in cluster 1 and the fact that the
363 majority of the rhythmic genes we identified within it are inhibitors of the central oscillator CIRCADIAN
364 CLOCK ASSOCIATED 1 / LATE ELONGATED HYPOCOTYL (CCA1/LHY), either directly such as PRR9, PRR7
365 (Farré & Liu, 2013) or indirectly such as PRR3 (via TOC1; Para et al., 2007) and LNK1 (via RVE8 and PRR5;
366 Kidokoro et al., 2023), it is possible that these genes are mediating the influence of the pathogen on the
367 circadian clock.

368 In the shoot PRR7 is activated in condition of low sugars by a mechanism involving the activation of the
369 sugar sensor SUCROSE NON FERMENTING RELATED KINASE 1 (SnRK1), itself phosphorylating the
370 transcription factor bZIP63 which activates PRR7 transcription (Frank et al., 2018). Interestingly, SnRK1

371 has been found to be the direct target of the recently described *P. brassicae*-specific effector protein
372 PBZF1 (W. Chen et al., 2021). SnRK1 is a central sensor of nutrient stress in plants (Han et al., 2024), and
373 the fact that this gene seems to be at the center of direct (i.e., via effectors) and indirect (i.e., via
374 changes in sugar levels) manipulation by *P. brassicae* argues for its pivotal role in the interaction. Recent
375 studies have shown that sucrose has an even higher importance in conveying circadian information in
376 the root, where sucrose pulses from the shoot regulate diel oscillations of PRR7 (and PRR9; Uemoto et
377 al., 2023). Unlike sucrose and trehalose-6-phosphate levels, plants do not regulate starch turnover based
378 on its abundance (Seki et al., 2017). As a result, the parasites direct consumption of sucrose and/or the
379 induction of amyloplastic storage could create a continuous flow of photosynthates towards the
380 infection-induced sink, disrupting the normal rhythmic pattern of sugar delivery to the root. This
381 scenario of a nutrient deprived tissue with consistent expression of PRR7 is further supported in our
382 study by the high expression of the "starvation gene" SKIP20 (a.k.a. KMD4 or At3g59940; Graf et al.,
383 2010) in infected roots.

384 Despite showing expression patterns like the one discussed above, GI and PIF4 are less clearly influenced
385 by sugar metabolism. Sucrose pulses in sugar-depleted condition in the dark are known to be able to re-
386 establish the oscillations of the circadian clock by post-transcriptionally stabilizing GI but they do not
387 change its expression levels (Dalchau et al., 2011; Haydon et al., 2017); whilst sucrose influences the
388 expression pattern of various PIFs, but not of PIF4 (Shor et al., 2017). GI is a plant specific circadian
389 protein promoting the transcription of thousands of genes and whose competitive interaction with PIF4
390 integrates endogenous oscillations with light and temperature in order to optimize growth (Nohales et
391 al., 2019; Park et al., 2020). Among the many processes influenced by GI, senescence is particularly
392 interesting, since it is also found in our GO term enrichment analysis of cluster 1 ("Plant organ
393 senescence"; "Leaf senescence"; Additional File 8) and prior studies have shown delayed senescence
394 when *GI* expression is suppressed (Thiruvengadam et al., 2015).

In our dataset, the established connection between circadian rhythms and senescence processes may be linked to the continuous expression of *GI* during the night, explaining the premature senescence and the yellowing of leaves observed as typical clubroot symptoms. GI nocturnal breakdown also regulates gibberellin mediated growth by allowing DELLA degradation and enabling the expression of downstream growth promoting genes (Nohales & Kay, 2019). The upregulation of *GI* in the night in our dataset might therefore be involved in disrupting the root growth (especially lateral root formation and main root elongation) by making cells insensitive to gibberellin (Shtin et al., 2022). Intriguingly, GI is also involved in stabilization of REPRESSOR OF GA (RGA; Park et al., 2020), itself inhibiting the gibberellin-induced transcription of PIF4 (another promoter of growth genes), which is instead upregulated in the night in infected plants. These results highlight the complexity of the influence of the circadian oscillator on downstream processes acting at the post-transcriptional level.

Conclusions

Overall, our exploration highlights a previously unrecognized nocturnal impact of *P. brassicae* on organellar dynamics and plant defences, and suggests a disruption of the host circadian processes. We provide target genes amenable to experimental validation, the necessary next step in order to answer questions on the time-specific cross-talk between *P. brassicae* and its host. Nocturnal manipulation of host organellar RNA editing by the parasite is likely to be linked to the diel oscillations in SA signalling and seemingly mediated by a subset of transcripts enriched in PPR encoding genes. The question remains whether PRR genes are a direct target of *P. brassicae* manipulation or whether the influence of the pathogen on their expression pattern is mediated by manipulation of SA signalling. Ongoing analyses of the diel changes in gene expression on the side of the parasite might help identifying time-specific effectors and help clarifying their targets. Furthermore, our investigation already revealed that circadian oscillations in gene expression (i.e., oscillations at a finer scale than the day and night) are altered by *P. brassicae*. In line with recent findings (Fu et al., 2025), the application of specific tools for the analysis of

differential rhythmicity to our dataset may further identify effectors allowing *P. brassicae* to hijack the circadian clock components to disrupt the physiology of the host plant.

Experimental procedures

Experimental setup & biological material

After germination, seedlings of *Arabidopsis thaliana* ecotype Col-0 obtained from the Seed Stock Centre (stock N1092, Nottingham, UK) were grown on a soil substrate (Einheitserde Type P, pH 5.8; Hermina Samen, Germany) mixed with sand (Sahara Spielsand; Hornbach Germany) in the ratio 4:1. This soil mixture was steam-sterilized prior to use for 120 minutes at 100 °C. All plants were grown in a Sanyo MLR-350H climate chamber at a temperature of 23°C during the day and 18°C during the night. The light/dark cycle was set to 12:12 hours, with a light intensity of 100 µmol. Genome-sequenced *Plasmodiophora brassicae* isolate e3 (Schwelm et al., 2015) obtained from Dr. Siemens (Fähling et al., 2004) was propagated on *B. rapa* var. *pekinensis* (ISP International Seed Processing GmbH, Quedlinburg, Germany) and pure spore suspensions were obtained as described in (Smolko et al., 2024). One week after germination, *A. thaliana* Col-0 plants were individually inoculated with 1 mL of *P. brassicae* isolate e3 spore suspension at a concentration of 10^6 spores/mL in 50 mM KH_2PO_4 buffer (pH 5.5, adjusted with K_2HPO_4) or with a mock inoculation of an equal amount of the same buffer. Healthy controls and infected plants were harvested 14 and 21 days after inoculation (DAI, Additional File 1 A and B), in each occasion at four different time points: two points during the “day” (5 hr 50’ and 10 hr 40’ after artificial dawn) and two points during the “night” (15 hr 30’ and 19 hr 20’; i.e., 3 hr 30’ and 7 hr 20’ after artificial dusk). The

442 time point 14 DAI was chosen as it marks the establishment of the secondary infection phase with
443 colonization of cortical tissue by metabolically active plasmodia and onset of visible symptoms in the
444 root (Liu et al., 2020). The second time point (i.e., 21 DAI) has been chosen as it matches the shift from
445 actively feeding plasmodia to resting spore production (Liu et al., 2020). Eight to twelve plants were
446 grown per each time point / treatment and harvested by pooling four plant roots in 1 mL ice-cold
447 RNAlater (Ambion, Austin, TX, USA) in 1.5 mL Eppendorf tubes. Samples were then left to rest overnight,
448 before removing and refreshing the RNAlater and storing them at -80°C until RNA extraction.

449 *RNA extraction & sequencing*

450 Samples in RNAlater were thawed on ice and one or two plant roots (when biomass from a single root
451 specimen was judged insufficient for RNA extraction) per each tube were transferred to ethanol-
452 sterilised and RNAseAway treated tin foil squares with equally treated steel tweezers (Additional File 1 C
453 and D). A root sample as described above constitute one replicate, and triplicate were selected and
454 processed per each time point, for infected and mock inoculated control plants at 14 DAI and 21 DAI,
455 resulting in a total of 48 processed roots (Additional File 2). Roots were carefully wrapped and snap-
456 frozen in liquid nitrogen before transferring them in pre-mixed bead matrix tubes (D1034-MX; Biozym,
457 Hessisch Oldendorf, Germany) amended with 200 µL IB buffer (SPLIT RNA Extraction Kit, Lexogen,
458 Vienna, Austria) to decrease the risk of RNA degradation and immediately homogenized with a FastPrep
459 bead mill (MP Biomedicals, Santa Ana, CA, USA) for 40 s at 60 ms^{-1} three times. After tissue disruption,
460 another 200 µL of ice cold IB buffer was added to the samples. The RNA extraction proceeded following
461 the protocol SPLIT RNA extraction of total RNA (SPLIT RNA Extraction Kit, Lexogen, Vienna, Austria) as
462 suggested by the manufacturer without further modifications. Assessment of the RNA extracts quality
463 and quantity was performed on an Agilent Bioanalyzer 2100 (Agilent Technologies, Palo Alto, CA, USA)
464 and Quantus fluorometer (Promega Corporation, Fitchburg, WI, USA). Strand-specific library preparation
465 was performed on poly-A-selected mRNA using a NEBNext Ultra II Directional RNA Library Prep Kit with

466 NEBNext Poly(A) mRNA Magnetic Isolation Module and NEBNext Multiplex Oligos for Illumina (New
467 England Biolabs, Ipswich, MA, USA). The quality and concentration of cDNA in the resulting libraries was
468 assessed on an Agilent Bioanalyzer 2100 and Quantus fluorometer, before paired-end sequencing (2x150
469 bp on a NovaSeq S1; Illumina, San Diego, CA, USA) at the VBCF NGS Unit (Vienna, Austria).

470 *Sequencing data processing*

471 Read quality was checked using FastQC (Andrews, 2010) and quality reports visualized in MultiQC v1.6
472 (Ewels et al., 2016) before and after read filtering and adapter trimming with Trim Galore v0.6.2 (quality
473 score threshold 30; https://zenodo.org/doi/10.5281/zenodo.5127898). To assign reads to the host plant
474 and the parasite, Bowtie2 v2.3.5.1 (Langmead & Salzberg, 2012) was used to map them against the
475 concatenated genomes of *Arabidopsis thaliana* (TAIR10; Lamesch et al., 2011) and *Plasmodiophora*
476 *brassicae* (Pldbra_eH_r1) with a "Place-to-go-based" approach as defined in (O'Keeffe & Jones, 2019).
477 Obtained read pools (separately for the host and the parasite) were assembled with Trinity v2.10.0 (in
478 genome guided mode; Grabherr et al., 2011)) and resulting transcripts annotated with Trinotate v3.2.1
479 (Bryant et al., 2017). Expression estimates were obtained by pre-aligning the reads to the transcripts
480 using STAR v2.7.1a (Dobin et al., 2013) and assigned to assembled transcript with Salmon (Patro et al.,
481 2017). Raw NGS sequences of the dataset obtained in this study are deposited in NCBI Sequence Read
482 Archive (SRA) under the BioProject accession number PRJNA1212907.

483 *Differential gene expression*

484 DESeq2 Bioconductor package (Love et al., 2014) in R (R Core Team, 2021) was used to estimate
485 differential gene expression. In order to detect differences in the response of plants to infection by *P.*
486 *brassicae* separately during the day and during the night, differentially expressed genes (DEGs) were
487 calculated on pooled counts. Briefly, read counts from all time points sampled during the day (i.e., 5 hr

488 50′ and 10 hr 40′ after artificial dawn) and during the night (15 hr 30′ and 19 hr 20′ after artificial dawn)
489 were pooled before further analyses.

490 This resulted in six replicates for each of the four conditions, as defined by the two factors "Condition"
491 (Infected or Control) and "Time point" (Day or Night; Additional file 2). An experimental design with two
492 factors and interaction was used for estimating the DEGs separately for 14 DAI and 21 DAI, thus resulting
493 in five comparisons: infected vs control in the day, infected vs control in the night, control in the night vs
494 in the day, infected in the night vs in the day and interaction. Genes were considered differentially
495 expressed when the adjusted p-value was ≤ 0.05 (Wald test p-value adjusted for multiple testing with
496 Benjamini–Hochberg correction) and a $\log_2$-fold change was ≤ −1 or ≥ 1.

497 *Principal component analysis and Venn diagram*

498 Principal component analysis (PCA) was calculated in the DESeq2 Bioconductor package in R (Love et al.,
499 2014) and further modified in ggplot2 (Wickham, 2010). The PCA was performed on variance stabilizing
500 transformed (vst) count data from the DESeqDataSet object, without taking into account the sample
501 information (i.e., blind=TRUE), as suggested by the DESeq2 manual. Venn diagrams on DEGs were
502 calculated in R with the Package VennDiagram (H. Chen, 2022).

503 *GO term over representation analyses*

504 ClusterProfiler (Wu et al., 2021) was used within R to perform gene ontology (GO) over-representation
505 tests using lists of DEGs in the comparisons between infected and healthy plants in the day and in the
506 night. Significance of the enriched GO categories was assessed by Fisher's exact test controlled for False
507 discovery rate (FDR) with Benjamini–Hochberg correction and the q-value cutoff was set to 0.05.
508 Because the RNA-seq strategy adopted was designed to measure all expressed mRNAs (total RNA
509 extraction followed by poly-A tail selection), the background gene list (or "universe") against which over-
510 representation was performed, was composed of a list of all protein coding genes from *A. thaliana*

TAIR10 genome release. The package GOplot (Walter et al., 2015) was used to combine expression data with functional categories. Using the function "circle_dat", the package was used to summarise and append to each enriched GO category an overall expression value (i.e., a z-score) calculated as follows:

$$z\ score = \frac{(\text{n° upregulated genes in GO } - \text{n° downregulated genes in GO })}{\sqrt{Total\ n°\ of\ genes\ in\ GO}}$$

The function "reduce_overlap" within the same package was used to eliminate all but one GO category sharing more than 25% of the genes before plotting the results with the function "GObubble".

Heatmap of gene expression levels

Genes whose differential expression levels were driven by the interaction between the factor "Time point" and the factor "Condition" were detected and their expression levels were visualised with heatmaps as implemented in the package pheatmap (Kolde, 2019) in R, on row-scaled, log-normalised read counts and with default "Euclidean" clustering method. All figures were further refined and finalized in Inkscape (Inkscape Project, 2020).

Author contributions

Experimental concept and design: SN, JLM. Wet lab work: SA, FB, AG, MH. Bioinformatics and statistical analysis: AG. Analysis of Results: AG, SN, SA, JLM, MH. Manuscript writing: AG, SN, SA, JLM. Figures and tables: AG. All authors read and approved the final manuscript.

Acknowledgements

We are grateful to Bettina Schneidhofer for her support in the wet lab. We would also like to thank the VBCF NGS Unit (www.vbcf.ac.at) in particular Carmen Czepe for her support during the sequencing and Nadine Tatto for her paramount contribution and continuous support with the bioinformatic analyses.

Conflict of interests

The authors declare that they have no competing interests. This article does not contain any studies with human or animal participants

Data availability statement

Raw NGS sequences of the dataset generated and analysed in the current study are available in NCBI Sequence Read Archive (SRA) under the BioProject accession number PRJNA1212907 or are available from the corresponding author on request.

Funding

This research was funded in whole by the Austrian Science Fund (FWF) [grant DOI:10.55776/Y801]. For open access purposes, the authors have applied a CC BY public copyright license to any author accepted manuscript version arising from this submission.

Supporting Information

Additional file 1. Above and below ground phenotypical traits of infected and control plants at 14 and 21 DAI.

Additional file 2. Detailed overview of the samples sequenced in this study.

Additional file 3. PCA on control *A. thaliana* plants, showing the decreased influence of the temporal factor with plant age.

Additional file 4. Volcano plot showing the number of DEGs in the day and night in infected *A. thaliana* plants 14 DAI.

Additional file 5. Volcano plot showing the number of DEGs in the day and night in infected *A. thaliana* plants 21 DAI.

Additional file 6. GO categories enriched in DEGs in *A. thaliana* roots 14 DAI infected by *P. brassicae.*

Additional file 7. GO categories enriched in DEGs in *A. thaliana* roots 21 DAI infected by *P. brassicae.*

Additional file 8. GO terms overrepresentation analysis of clusters of DEGs driven by the interaction between infection and time of the day 14 DAI.

Additional file 9. GO terms overrepresentation analysis of clusters of DEGs driven by the interaction between infection and time of the day 21 DAI.

557 **Additional file 10.** Enriched GO terms and corresponding genes underpinning figure 2 and 3 before data
558 reduction.

559

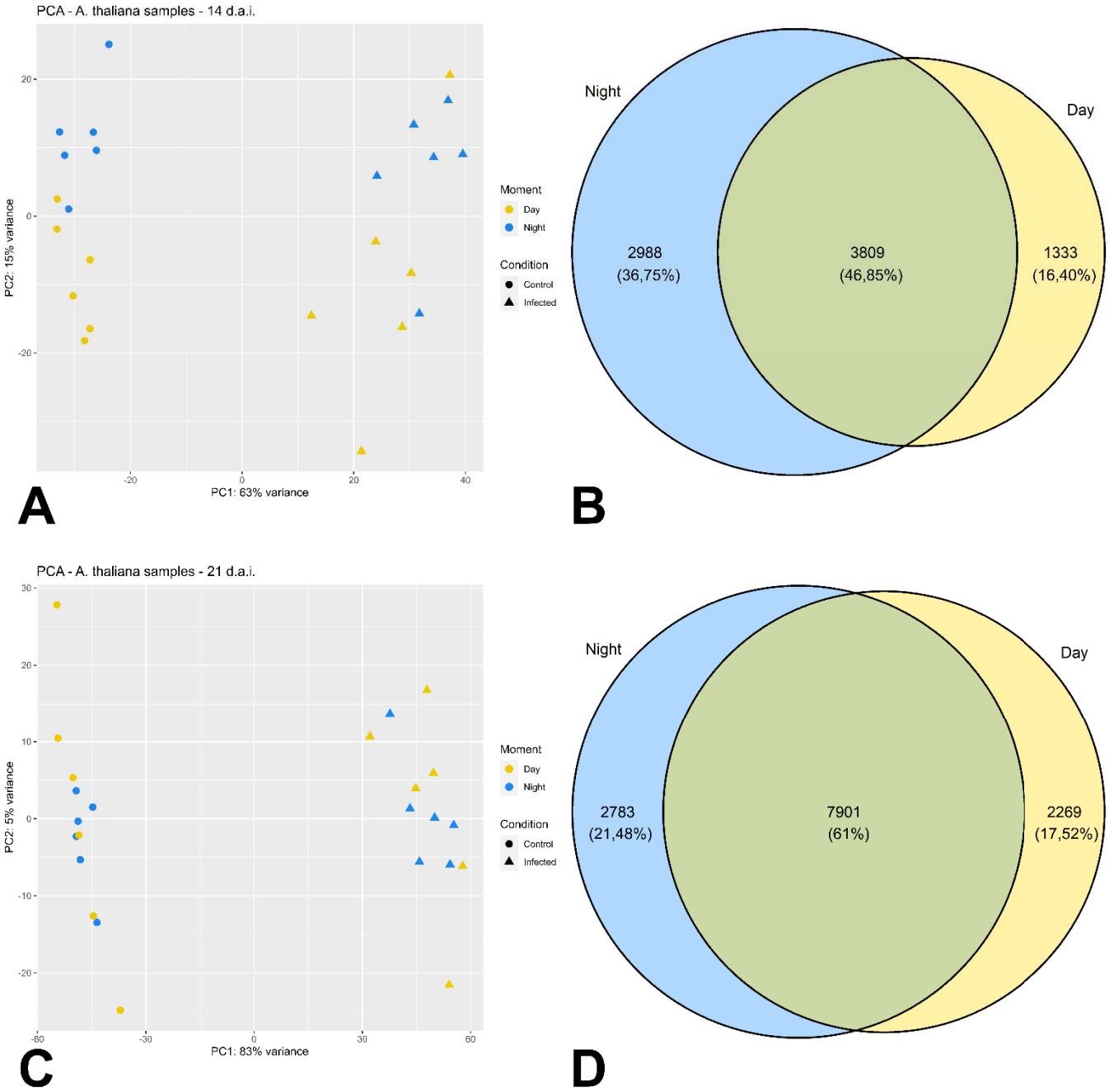

560

561 *Fig. 1 Day/night-informed overview of gene expression in samples of A. thaliana roots 14 DAI (A, B) and 21 DAI (C, D) with P.*
562 *brassicae. A and C, PCA of A. thaliana root samples structured by gene expression estimates (i.e., vst counts). B and D,*
563 *Proportions of DE genes between infected and healthy A. thaliana roots assigned to the day, night or both.*

564

565

566 *Fig. 2 GO bubble chart of GO categories enriched in DEGs in infected A. thaliana roots during the day (A, yellow) and night (B,*
567 *blue) 14 DAI by P. brassicae. The bubbles are arranged according to their overall expression level or z-score on the x axis and*
568 *according to the negative logarithmic scale of the adjusted p-value on the y axis. The bubble size is proportional to the gene*
569 *counts within each category. The significance threshold of adjusted p-value < 0,05 (1,3 in -log10 scale) is represented by coloured*
570 *lines parallel to the x axis (orange in the day and turquoise in the night).*

571

572

573

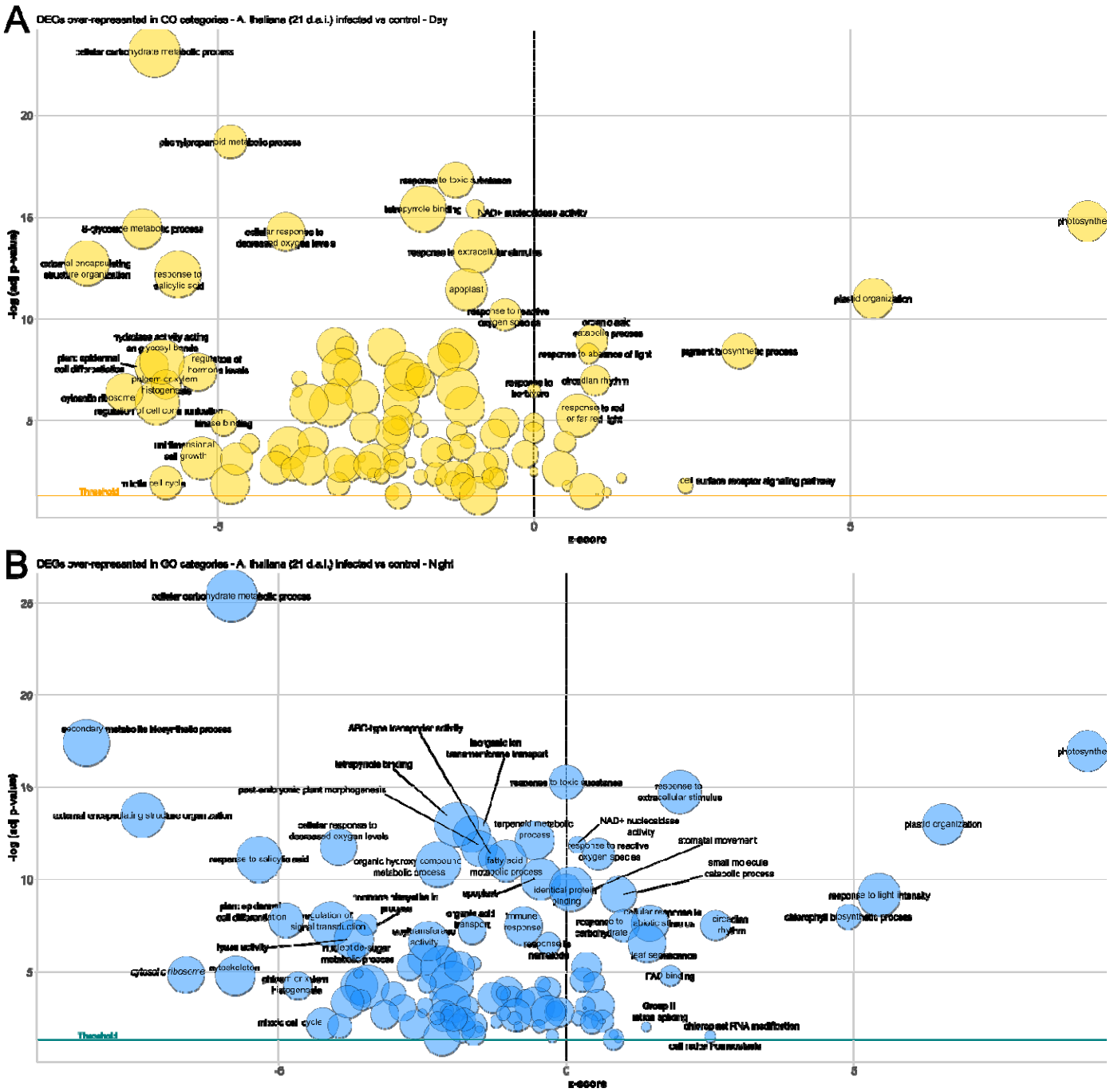

Fig. 3 GO bubble chart of GO categories enriched in DEGs in infected A. thaliana roots during the day (top, yellow) and night (blue, bottom) 21 DAI by P. brassicae. The bubbles are arranged according to their overall expression level or z-score on the x axis and according to the negative logarithmic scale of the adjusted p-value on the y axis. The bubble size is proportional to the gene counts within each category. The significance threshold of adjusted p-value < 0,05 (1,3 in -log10 scale) is represented by coloured lines parallel to the x axis (orange in the day and turquoise in the night).

Fig. 4 Heatmap highlighting DEGs explained by the interaction between infection and time of the day as detected in infected A .thaliana roots 14 DAI The row-normalised and log transformed gene counts are shown for each sample separately. The status of each sample is described by a combination of green (control plant) or purple (infected plant) and yellow (day) or (blue) bars. DEGs with similar patterns of expression have been grouped in 8 clusters (numbers in white boxes).

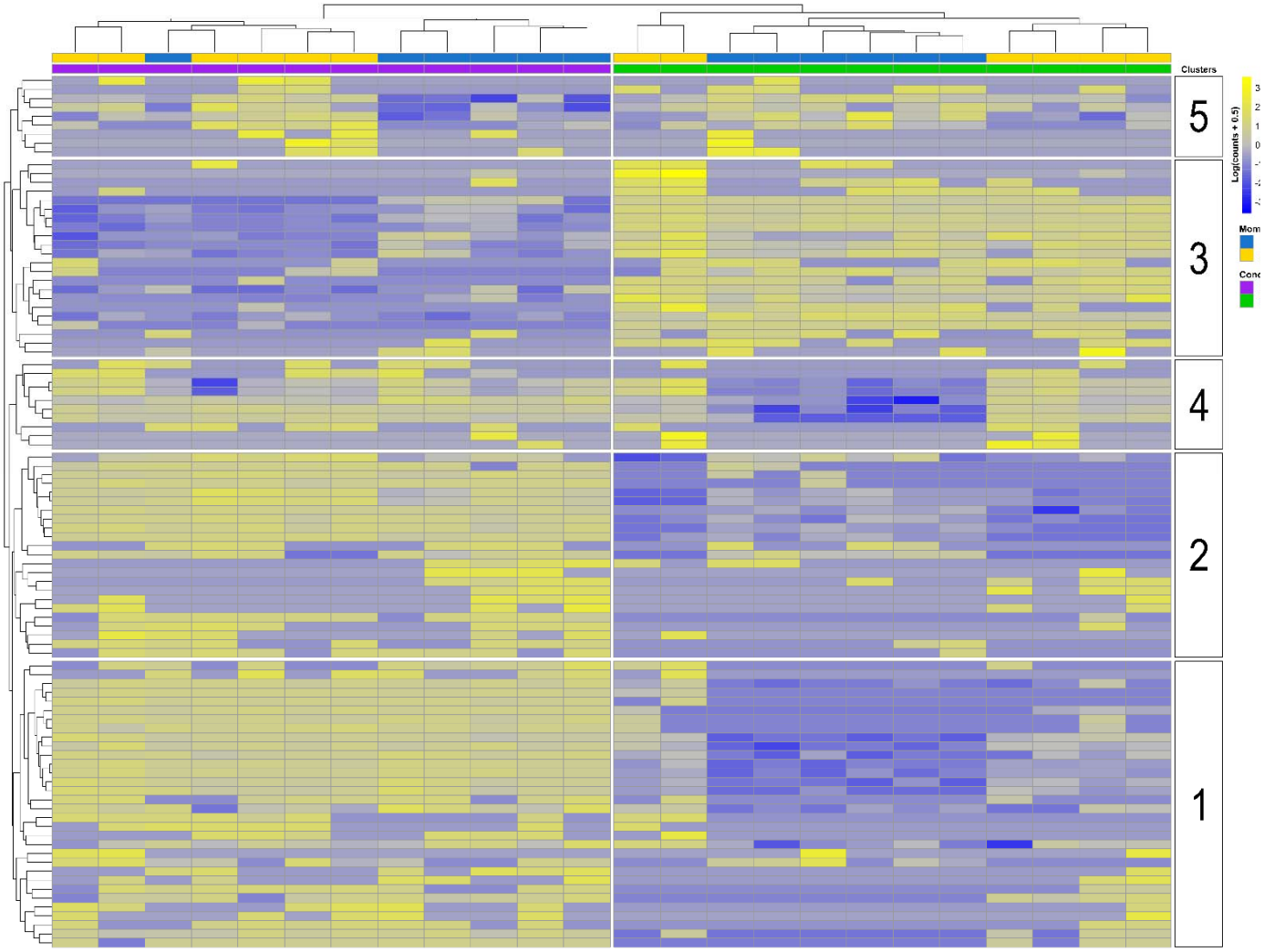

Fig. 5: Heatmap highlighting DEGs explained by the interaction between infection and time of the day as detected in infected A .thaliana roots 21 DAI The row-normalised and log transformed gene counts are shown for each sample separately. The status of each sample is described by a combination of green (control plant) or purple (infected plant) and yellow (day) or (blue) bars. DEGs with similar patterns of expression have been grouped in 5 clusters (numbers in white boxes).

References

Agarwal, A., Kaul, V., Faggian, R., Rookes, J. E., Ludwig-Müller, J., & Cahill, D. M. (2011). Analysis of global host gene expression during the primary phase of the Arabidopsis thalianaPlasmodiophora brassicae interaction. *Functional Plant Biology*, *38*(6), 462–478. https://doi.org/10.1071/FP11026

Andrews, S. (2010). *FastQC A Quality Control tool for High Throughput Sequence Data*. Http://Www.Bioinformatics.Babraham.Ac.Uk/Projects/Fastqc/.

Barkan, A., & Small, I. (2014). Pentatricopeptide repeat proteins in plants. *Annual Review of Plant Biology*, *65*, 415–442. https://doi.org/10.1146/annurev-arplant-050213-040159

Bauters, L., Stojilković, B., & Gheysen, G. (2021). Pathogens pulling the strings: Effectors manipulating salicylic acid and phenylpropanoid biosynthesis in plants. In *Molecular Plant Pathology* (Vol. 22, Issue 11, pp. 1436–1448). John Wiley and Sons Inc. https://doi.org/10.1111/mpp.13123

Bryant, D. M., Johnson, K., DiTommaso, T., Tickle, T., Couger, M. B., Payzin-Dogru, D., Lee, T. J., Leigh, N. D., Kuo, T. H., Davis, F. G., Bateman, J., Bryant, S., Guzikowski, A. R., Tsai, S. L., Coyne, S., Ye, W. W., Freeman, R. M., Peshkin, L., Tabin, C. J., … Whited, J. L. (2017). A Tissue-Mapped Axolotl De Novo Transcriptome Enables Identification of Limb Regeneration Factors. *Cell Reports*, *18*(3), 762–776. https://doi.org/10.1016/j.celrep.2016.12.063

Bustillo-Avendaño, E., Serrano-Ron, L., & Moreno-Risueno, M. A. (2022). The Root Clock as a Signal Integrator System: Ensuring Balance for Survival. *Frontiers in Plant Science*, *13*(May). https://doi.org/10.3389/fpls.2022.886700

Chen, H. (2022). *VennDiagram: Generate High-Resolution Venn and Euler Plots*.

Chen, J. Y., Wen, P. F., Kong, W. F., Pan, Q. H., Zhan, J. C., Li, J. M., Wan, S. B., & Huang, W. D. (2006). Effect of salicylic acid on phenylpropanoids and phenylalanine ammonia-lyase in harvested grape berries. *Postharvest Biology and Technology*, *40*(1), 64–72. https://doi.org/10.1016/j.postharvbio.2005.12.017

Chen, W., Li, Y., Yan, R., Ren, L., Liu, F., Zeng, L., Sun, S., Yang, H., Chen, K., Xu, L., Liu, L., Fang, X., & Liu, S. (2021). SnRK1.1-mediated resistance of Arabidopsis thaliana to clubroot disease is inhibited by the novel Plasmodiophora brassicae effector PBZF1. *Molecular Plant Pathology*, *22*(9), 1057–1069. https://doi.org/10.1111/mpp.13095

Ciaghi, S., Schwelm, A., & Neuhauser, S. (2019). Transcriptomic response in symptomless roots of clubroot infected kohlrabi (Brassica oleracea var. gongylodes) mirrors resistant plants. *BMC Plant Biology*, *19*(1), 1–14. https://doi.org/10.1186/s12870-019-1902-z

Dalchau, N., Baek, S. J., Briggs, H. M., Robertson, F. C., Dodd, A. N., Gardner, M. J., Stancombe, M. A., Haydon, M. J., Stan, G. B., Gonçalves, J. M., & Webb, A. A. R. (2011). The circadian oscillator gene GIGANTEA mediates a long-term response of the Arabidopsis thaliana circadian clock to sucrose. *Proceedings of the National Academy of Sciences of the United States of America*, *108*(12), 5104–5109. https://doi.org/10.1073/pnas.1015452108

640 Davis, W., Endo, M., & Locke, J. C. W. (2022). Spatially specific mechanisms and functions of the plant
641 circadian clock. *Plant Physiology*, *190*(2), 938–951. https://doi.org/10.1093/plphys/kiac236

642 Dekhuijzen, H. M. (1981). The Occurrence of Free and Bound Cytokinins in Plasmodia of Plasmodiophora
643 brassicae Isolated from Tissue Cultures of Clubroots. *Plant Cell Reports*, *213*, 29–30.

644 Dekhuijzen, H. M., & Overeem, J. C. (1971). The role of cytokinins in clubroot formation. *Physiological*
645 *Plant Pathology*, *1*(2), 151–161. https://doi.org/10.1016/0048-4059(71)90024-5

646 Devos, S., Laukens, K., Deckers, P., Van Der Straeten, D., Beeckman, T., Inzé, D., Van Onckelen, H.,
647 Witters, E., & Prinsen, E. (2006). A hormone and proteome approach to picturing the initial
648 metabolic events during Plasmodiophora brassicae infection on Arabidopsis. *Molecular Plant-*
649 *Microbe Interactions*, *19*(12), 1431–1443. https://doi.org/10.1094/MPMI-19-1431

650 Devos, S., Vissenberg, K., Verbelen, J. P., & Prinsen, E. (2005). Infection of Chinese cabbage by
651 Plasmodiophora brassicae leads to a stimulation of plant growth: Impacts on cell wall metabolism
652 and hormone balance. *New Phytologist*, *166*(1), 241–250. https://doi.org/10.1111/j.1469-
653 8137.2004.01304.x

654 Dixon, G. R. (2009). The occurrence and economic impact of plasmodiophora brassicae and clubroot
655 disease. *Journal of Plant Growth Regulation*, *28*(3), 194–202. https://doi.org/10.1007/s00344-009-
656 9090-y

657 Djavaheri, M., Ma, L., Klessig, D. F., Mithöfer, A., Gropp, G., & Borhan, H. (2019). Mimicking the host
658 regulation of salicylic acid: A virulence strategy by the clubroot pathogen plasmodiophora
659 brassicae. *Molecular Plant-Microbe Interactions*, *32*(3), 296–305. https://doi.org/10.1094/MPMI-
660 07-18-0192-R

661 Dobin, A., Davis, C. A., Schlesinger, F., Drenkow, J., Zaleski, C., Jha, S., Batut, P., Chaisson, M., & Gingeras,
662 T. R. (2013). STAR: Ultrafast universal RNA-seq aligner. *Bioinformatics*, *29*(1), 15–21.
663 https://doi.org/10.1093/bioinformatics/bts635

664 Dong, N. Q., & Lin, H. X. (2021). Contribution of phenylpropanoid metabolism to plant development and
665 plant–environment interactions. *Journal of Integrative Plant Biology*, *63*(1), 180–209.
666 https://doi.org/10.1111/jipb.13054

667 Duda, J. C., Drenda, C., Kästel, H., Rahnenführer, J., & Kappenberg, F. (2023). Benefit of using interaction
668 effects for the analysis of high-dimensional time-response or dose-response data for two-group
669 comparisons. *Scientific Reports*, *13*(1), 1–12. https://doi.org/10.1038/s41598-023-47057-0

670 Durand, M., Mainson, D., Porcheron, B., Maurousset, L., Lemoine, R., & Pourtau, N. (2018). Carbon
671 source–sink relationship in Arabidopsis thaliana: the role of sucrose transporters. *Planta*, *247*(3),
672 587–611. https://doi.org/10.1007/s00425-017-2807-4

673 Ehrary, A., Rosas, M., Carpinelli, S., Davalos, O., Cowling, C., Fernandez, F., & Escobar, M. (2020).
674 Glutaredoxin AtGRXS8 represses transcriptional and developmental responses to nitrate in
675 Arabidopsis thaliana roots. *Plant Direct*, *4*(6). https://doi.org/10.1002/pld3.227

676 Enami, K., Ozawa, T., Motohashi, N., Nakamura, M., Tanaka, K., & Hanaoka, M. (2011). Plastid-to-nucleus
677 retrograde signals are essential for the expression of nuclear starch biosynthesis genes during

amyloplast differentiation in tobacco BY-2 cultured cells. *Plant Physiology*, *157*(1), 518–530. https://doi.org/10.1104/pp.111.178897

Ewels, P., Magnusson, M., Lundin, S., & Käller, M. (2016). MultiQC: Summarize analysis results for multiple tools and samples in a single report. *Bioinformatics*, *32*(19), 3047–3048. https://doi.org/10.1093/bioinformatics/btw354

Fähling, M., Graf, H., & Siemens, J. (2004). Characterization of a Single-Spore Isolate Population of Plasmodiophora brassicae Resulting from a Single Club. *Journal of Phytopathology*, *152*, 438–444.

Farré, E. M., & Liu, T. (2013). The PRR family of transcriptional regulators reflects the complexity and evolution of plant circadian clocks. *Current Opinion in Plant Biology*, *16*(5), 621–629. https://doi.org/10.1016/j.pbi.2013.06.015

Frank, A., Matiolli, C. C., Viana, A. J. C., Hearn, T. J., Kusakina, J., Belbin, F. E., Wells Newman, D., Yochikawa, A., Cano-Ramirez, D. L., Chembath, A., Cragg-Barber, K., Haydon, M. J., Hotta, C. T., Vincentz, M., Webb, A. A. R., & Dodd, A. N. (2018). Circadian Entrainment in Arabidopsis by the Sugar-Responsive Transcription Factor bZIP63. *Current Biology*, *28*(16), 2597-2606.e6. https://doi.org/10.1016/j.cub.2018.05.092

Fraser, O. J. P., Cargill, S. J., Spoel, S. H., & van Ooijen, G. (2024). Crosstalk between salicylic acid signalling and the circadian clock promotes an effective immune response in plants. *Npj Biological Timing and Sleep*, *1*(1). https://doi.org/10.1038/s44323-024-00006-0

Fu, M., Zhou, Y., Zhang, X., Yang, K., Xu, Y., Wang, X., Chen, Z., Wang, Y., Shi, Y., Ma, L., Liu, H., Deng, Y., Cheng, S., Chu, J., Song, J., Sun, T., Wang, Y., Wang, W., & Zhou, M. (2025). A pathogen effector HaRxL10 hijacks the circadian clock component CHE to perturb both plant development and immunity. *Nature Communications* , *16*(1). https://doi.org/10.1038/s41467-025-56787-w

Galindo-González, L., Manolii, V., Hwang, S. F., & Strelkov, S. E. (2020). Response of Brassica napus to Plasmodiophora brassicae Involves Salicylic Acid-Mediated Immunity: An RNA-Seq-Based Study. *Frontiers in Plant Science*, *11*(July), 1–20. https://doi.org/10.3389/fpls.2020.01025

García-Andrade, J., Ramírez, V., López, A., & Vera, P. (2013). Mediated Plastid RNA Editing in Plant Immunity. *PLoS Pathogens*, *9*(10). https://doi.org/10.1371/journal.ppat.1003713

Garvetto, A., Murúa, P., Kirchmair, M., Salvenmoser, W., Hittorf, M., Ciaghi, S., Harikrishnan, S. L., Gachon, C. M. M., Burns, J. A., & Neuhauser, S. (2023). Phagocytosis underpins the biotrophic lifestyle of intracellular parasites in the class Phytomyxea (Rhizaria). *New Phytologist*, *238*(5), 2130–2143. https://doi.org/10.1111/nph.18828

Goodspeed, D., Chehab, E. W., Min-Venditti, A., Braam, J., & Covington, M. F. (2012). Arabidopsis synchronizes jasmonate-mediated defense with insect circadian behavior. *Proceedings of the National Academy of Sciences of the United States of America*, *109*(12), 4674–4677. https://doi.org/10.1073/pnas.1116368109

Grabherr, M. G., Haas, B. J., Yassour, M., Levin, J. Z., Thompson, D. A., Amit, I., Adiconis, X., Fan, L., Raychowdhury, R., Zeng, Q., Chen, Z., Mauceli, E., Hacohen, N., Gnirke, A., Rhind, N., di Palma, F., Birren, B. W., Nusbaum, C., Lindblad-Toh, K., … Regev, A. (2011). Full-length transcriptome

assembly from RNA-Seq data without a reference genome. *Nature Biotechnology*, *29*(7), 644–652. https://doi.org/10.1038/nbt.1883

Graf, A., Schlereth, A., Stitt, M., & Smith, A. M. (2010). Circadian control of carbohydrate availability for growth in Arabidopsis plants at night. *Proceedings of the National Academy of Sciences of the United States of America*, *107*(20), 9458–9463. https://doi.org/10.1073/pnas.0914299107

Gravot, A., Deleu, C., Wagner, G., Lariagon, C., Lugan, R., Todd, C., Wendehenne, D., Delourme, R., Bouchereau, A., & Manzanares-Dauleux, M. J. (2012). Arginase induction represses gall development during clubroot infection in arabidopsis. *Plant and Cell Physiology*, *53*(5), 901–911. https://doi.org/10.1093/pcp/pcs037

Gravot, A., Richard, G., Lime, T., Lemarié, S., Jubault, M., Lariagon, C., Lemoine, J., Vicente, J., Robert-Seilaniantz, A., Holdsworth, M. J., & Manzanares-Dauleux, M. J. (2016). Hypoxia response in Arabidopsis roots infected by Plasmodiophora brassicae supports the development of clubroot. *BMC Plant Biology*, *16*(1), 1–10. https://doi.org/10.1186/s12870-016-0941-y

Grsic-Rausch, S., Kobelt, P., Siemens, J. M., Bischoff, M., & Ludwig-Müller, J. (2000). Expression and localization of nitrilase during symptom development of the clubroot disease in Arabidopsis. *Plant Physiology*, *122*(2), 369–378. https://doi.org/10.1104/pp.122.2.369

Han, C., Wang, H., Shi, W., & Bai, M.-Y. (2024). The molecular associations between the SnRK1 complex and carbon/nitrogen metabolism in plants. *New Crops*, *1*(December 2023), 100008. https://doi.org/10.1016/j.ncrops.2023.12.003

Haydon, M. J., Mielczarek, O., Frank, A., Román, Á., & Webb, A. A. R. (2017). Sucrose and ethylene signaling interact to modulate the circadian clock. *Plant Physiology*, *175*(2), 947–958. https://doi.org/10.1104/pp.17.00592

Henriques, R., Papdi, C., Ahmad, Z., & Bögre, L. (2018). Circadian Regulation of Plant Growth. *Annual Plant Reviews Online*, *1*, 675–704. https://doi.org/10.1002/9781119312994.apr0655

Hurný, A., Cuesta, C., Cavallari, N., Ötvös, K., Duclercq, J., Dokládal, L., Montesinos, J. C., Gallemí, M., Semerádová, H., Rauter, T., Stenzel, I., Persiau, G., Benade, F., Bhalearo, R., Sýkorová, E., Gorzsás, A., Sechet, J., Mouille, G., Heilmann, I., … Benková, E. (2020). SYNERGISTIC ON AUXIN AND CYTOKININ 1 positively regulates growth and attenuates soil pathogen resistance. *Nature Communications*, *11*(1). https://doi.org/10.1038/s41467-020-15895-5

Inkscape Project. (2020). *Inkscape*. Retrieved from https://inkscape.org.

Irani, S., Trost, B., Waldner, M., Nayidu, N., Tu, J., Kusalik, A. J., Todd, C. D., Wei, Y., & Bonham-Smith, P. C. (2018). Transcriptome analysis of response to Plasmodiophora brassicae infection in the Arabidopsis shoot and root. *BMC Genomics*, *19*(1), 23. https://doi.org/10.1186/s12864-017-4426-7

Javed, M. A., Schwelm, A., Zamani-Noor, N., Salih, R., Silvestre Vañó, M., Wu, J., González García, M., Heick, T. M., Luo, C., Prakash, P., & Pérez-López, E. (2023). The clubroot pathogen Plasmodiophora brassicae: A profile update. *Molecular Plant Pathology*, *24*(2), 89–106. https://doi.org/10.1111/mpp.13283

Jayasinghege, C. P. A., Ozga, J. A., Manolii, V. P., Hwang, S. F., & Strelkov, S. E. (2023). Impact of Susceptibility on Plant Hormonal Composition during Clubroot Disease Development in Canola (Brassica napus). *Plants*, *12*(16). https://doi.org/10.3390/plants12162899

Kageyama, K., & Asano, T. (2009). Life cycle of plasmodiophora brassicae. *Journal of Plant Growth Regulation*, *28*(3), 203–211. https://doi.org/10.1007/s00344-009-9101-z

Karapetyan, S., & Dong, X. (2018). Redox and the circadian clock in plant immunity: A balancing act. In *Free Radical Biology and Medicine* (Vol. 119, pp. 56–61). Elsevier Inc. https://doi.org/10.1016/j.freeradbiomed.2017.12.024

Keen, N. T., & Williams, P. H. (1969). Translocation of Sugars into Infected Cabbage Tissues during Clubroot Development. *Plant Physiology*, *44*(5), 748–754.

Kidokoro, S., Konoura, I., Soma, F., Suzuki, T., Miyakawa, M., Shinozaki, K., & Yamaguchi-Shinozaki, K. (2023). Clock-regulated coactivators selectively control gene expression in response to different temperature stress conditions in Arabidopsis. *Proceedings of the National Academy of Sciences*, *120*(16), 1–11. https://doi.org/10.1073/pnas

Kim, H., & Hong, S. (2019). Role of the circadian clock in fine-tuning the process of leaf senescence in plants. *Translational Medicine of Aging*, *3*(2019), 26–30. https://doi.org/10.1016/j.tma.2018.12.001

Kolde, R. (2019). *pheatmap: Pretty Heatmaps*.

Kunkel, L. (1918). Tissue invasion by Plasmodiophora brassicae. *Journal of Agricultural Research*, *12*(543), 543–572.

Lamesch, P., Berardini, T. Z., Li, D., Swarbreck, D., Wilks, C., Sasidharan, R., Muller, R., Dreher, K., Alexander, D. L., Garcia-Hernandez, M., Karthikeyan, A. S., Lee, C. H., Nelson, W. D., Ploetz, L., Singh, S., Wensel, A., & Huala, E. (2011). The Arabidopsis Information Resource (TAIR): Improved gene annotation and new tools. *Nucleic Acids Research*, *40*(D1), 1202–1210. https://doi.org/10.1093/nar/gkr1090

Langmead, B., & Salzberg, S. L. (2012). Fast gapped-read alignment with Bowtie 2. *Nature Methods*, *9*(4), 357–359. https://doi.org/10.1038/nmeth.1923

Lee, J., Kang, M. H., Kim, J. Y., & Lim, P. O. (2021). The Role of Light and Circadian Clock in Regulation of Leaf Senescence. *Frontiers in Plant Science*, *12*(April). https://doi.org/10.3389/fpls.2021.669170

Lemarié, S., Robert-Seilaniantz, A., Lariagon, C., Lemoine, J., Marnet, N., Jubault, M., Manzanares-Dauleux, M. J., & Gravot, A. (2015). Both the Jasmonic Acid and the Salicylic Acid Pathways Contribute to Resistance to the Biotrophic Clubroot Agent Plasmodiophora brassicae in Arabidopsis. *Plant and Cell Physiology*, *56*(11), 2158–2168. https://doi.org/10.1093/pcp/pcv127

Liebers, M., Grübler, B., Chevalier, F., Lerbs-Mache, S., Merendino, L., Blanvillain, R., & Pfannschmidt, T. (2017). Regulatory shifts in plastid transcription play a key role in morphological conversions of plastids during plant development. *Frontiers in Plant Science*, *8*. https://doi.org/10.3389/fpls.2017.00023

789 Liu, L., Qin, L., Zhou, Z., Hendriks, W. G. H. M., Liu, S., & Wei, Y. (2020). Refining the life cycle of
790 Plasmodiophora brassicae. *Phytopathology*, *110*(10), 1704–1712. https://doi.org/10.1094/PHYTO-
791 02-20-0029-R

792 Love, M. I., Huber, W., & Anders, S. (2014). Moderated estimation of fold change and dispersion for RNA-
793 seq data with DESeq2. *Genome Biology*, *15*(12), 1–21. https://doi.org/10.1186/s13059-014-0550-8

794 Lovelock, D. A., Donald, C. E., Conlan, X. A., & Cahill, D. M. (2013). Salicylic acid suppression of clubroot in
795 broccoli (Brassicae oleracea var. italica) caused by the obligate biotroph Plasmodiophora brassicae.
796 *Australasian Plant Pathology*, *42*(2), 141–153. https://doi.org/10.1007/s13313-012-0167-x

797 Lovelock, D. A., Šola, I., Marschollek, S., Donald, C. E., Rusak, G., van Pée, K. H., Ludwig-Müller, J., &
798 Cahill, D. M. (2016). Analysis of salicylic acid-dependent pathways in Arabidopsis thaliana following
799 infection with Plasmodiophora brassicae and the influence of salicylic acid on disease. *Molecular*
800 *Plant Pathology*, *17*(8), 1237–1251. https://doi.org/10.1111/mpp.12361

801 Lu, H., McClung, C. R., & Zhang, C. (2017). Tick Tock: Circadian Regulation of Plant Innate Immunity.
802 *Annual Review of Phytopathology*, *55*, 287–311. https://doi.org/10.1146/annurev-phyto-080516-
803 035451

804 Ludwig-Müller, J., Jülke, S., Geiß, K., Richter, F., Mithöfer, A., Šola, I., Rusak, G., Keenan, S., & Bulman, S.
805 (2015). A novel methyltransferase from the intracellular pathogen Plasmodiophora brassicae
806 methylates salicylic acid. *Molecular Plant Pathology*, *16*(4), 349–364.
807 https://doi.org/10.1111/mpp.12185

808 Ludwig-Müller, J., Prinsen, E., Rolfe, S. A., & Scholes, J. D. (2009). Metabolism and plant hormone action
809 during clubroot disease. *Journal of Plant Growth Regulation*, *28*(3), 229–244.
810 https://doi.org/10.1007/s00344-009-9089-4

811 Ma, Y., Choi, S. R., Wang, Y., Chhapekar, S. S., Zhang, X., Wang, Y., Zhang, X., Zhu, M., Liu, D., Zuo, Z., Yan,
812 X., Gan, C., Zhao, D., Liang, Y., Pang, W., & Lim, Y. P. (2022). Starch content changes and
813 metabolism-related gene regulation of Chinese cabbage synergistically induced by Plasmodiophora
814 brassicae infection. *Horticulture Research*.

815 Malinowski, R., Novák, O., Borhan, M. H., Spíchal, L., Strnad, M., & Rolfe, S. A. (2016). The role of
816 cytokinins in clubroot disease. *European Journal of Plant Pathology*, *145*(3), 543–557.
817 https://doi.org/10.1007/s10658-015-0845-y

818 Malinowski, R., Truman, W., & Blicharz, S. (2019). Genius architect or clever thief — How
819 Plasmodiophora brassicae reprograms host development to establish a pathogen-oriented
820 physiological sink. *Molecular Plant-Microbe Interactions*, *32*(10), 1259–1266.
821 https://doi.org/10.1094/MPMI-03-19-0069-CR

822 Meinke, D. W., Cherry, J. M., Dean, C., Rounsley, S. D., & Koornneef, M. (1998). Arabidopsis thaliana: A
823 model plant for genome analysis. *Science*, *282*(5389).
824 https://doi.org/10.1126/science.282.5389.662

825 Mencia, R., Céccoli, G., Fabro, G., Torti, P., Colombatti, F., Ludwig-Müller, J., Alvarez, M. E., & Welchen, E.
826 (2020). OXR2 increases plant defense against a hemibiotrophic pathogen via the salicylic acid
827 pathway. *Plant Physiology*, *184*(2), 1112–1127. https://doi.org/10.1104/pp.19.01351

828 Mencia, R., Welchen, E., Auer, S., & Ludwig-Müller, J. (2022). A Novel Target (Oxidation Resistant 2) in
829 Arabidopsis thaliana to Reduce Clubroot Disease Symptoms via the Salicylic Acid Pathway without
830 Growth Penalties. *Horticulturae*, *8*(1). https://doi.org/10.3390/horticulturae8010009

831 Mora-García, S., de Leone, M. J., & Yanovsky, M. (2017). Time to grow: circadian regulation of growth
832 and metabolism in photosynthetic organisms. *Current Opinion in Plant Biology*, *35*, 84–90.
833 https://doi.org/10.1016/j.pbi.2016.11.009

834 Mortada, M., Xiong, L., & Mas, P. (2024). Dissecting the complexity of local and systemic circadian
835 communication in plants. *Npj Biological Timing and Sleep*, *1*(1), 1–7.
836 https://doi.org/10.1038/s44323-024-00003-3

837 Motta, F. C., McGoff, K., Moseley, R. C., Cho, C. Y., Kelliher, C. M., Smith, L. M., Ortiz, M. S., Leman, A. R.,
838 Campione, S. A., Devos, N., Chaorattanakawee, S., Uthaimongkol, N., Kuntawunginn, W.,
839 Thongpiam, C., Thamnurak, C., Arsanok, M., Wojnarski, M., Vanchayangkul, P., Boonyalai, N., …
840 Haase, S. B. (2023). The parasite intraerythrocytic cycle and human circadian cycle are coupled
841 during malaria infection. *Proceedings of the National Academy of Sciences of the United States of*
842 *America*, *120*(24). https://doi.org/10.1073/pnas.2216522120

843 Müller, P., & Hilgenberg, W. (1986). Isomers of zeatin and zeatin riboside in clubroot tissue: evidence for
844 trans-zeatin biosynthesis by Plasmodiophora brassicae. *Physiologia Plantarum*, *66*(2), 245–250.
845 https://doi.org/10.1111/j.1399-3054.1986.tb02415.x

846 Neuhaus, K., Grsic-Rausch, S., Sauerteig, S., & Ludwig-Müller, J. (2000). Arabidopsis plants transformed
847 with nitrilase 1 or 2 in antisense direction are delayed in clubroot development. *Journal of Plant*
848 *Physiology*, *156*(5–6), 756–761. https://doi.org/10.1016/S0176-1617(00)80243-6

849 Nohales, M. A., & Kay, S. A. (2019). GIGANTEA gates gibberellin signaling through stabilization of the
850 DELLA proteins in Arabidopsis. *Proceedings of the National Academy of Sciences of the United*
851 *States of America*, *116*(43), 21893–21899. https://doi.org/10.1073/pnas.1913532116

852 Nohales, M. A., Liu, W., Duffy, T., Nozue, K., Sawa, M., Pruneda-Paz, J. L., Maloof, J. N., Jacobsen, S. E., &
853 Kay, S. A. (2019). Multi-level Modulation of Light Signaling by GIGANTEA Regulates Both the Output
854 and Pace of the Circadian Clock. *Developmental Cell*, *49*(6), 840-851.e8.
855 https://doi.org/10.1016/j.devcel.2019.04.030

856 O'Keeffe, K. R., & Jones, C. D. (2019). Challenges and solutions for analysing dual RNA-seq data for non-
857 model host–pathogen systems. *Methods in Ecology and Evolution*, *10*(3), 401–414.
858 https://doi.org/10.1111/2041-210X.13135

859 Olszak, M., Truman, W., Stefanowicz, K., Sliwinska, E., Ito, M., Walerowski, P., Rolfe, S., & Malinowski, R.
860 (2019). Transcriptional profiling identifies critical steps of cell cycle reprogramming necessary for
861 Plasmodiophora brassicae-driven gall formation in Arabidopsis. *Plant Journal*, *97*(4), 715–729.
862 https://doi.org/10.1111/tpj.14156

863 Para, A., Farré, E. M., Imaizumi, T., Pruneda-Paz, J. L., Harmon, F. G., & Kay, S. A. (2007). PRR3 is a
864 vascular regulator of TOC1 stability in the Arabidopsis circadian clock. *Plant Cell*, *19*(11), 3462–
865 3473. https://doi.org/10.1105/tpc.107.054775

Park, Y. J., Kim, J. Y., Lee, J. H., Lee, B. D., Paek, N. C., & Park, C. M. (2020). GIGANTEA Shapes the Photoperiodic Rhythms of Thermomorphogenic Growth in Arabidopsis. *Molecular Plant*, *13*(3), 459–470. https://doi.org/10.1016/j.molp.2020.01.003

Patro, R., Duggal, G., Love, M. I., Irizarry, R. A., & Kingsford, C. (2017). Salmon provides fast and bias-aware quantification of transcript expression. *Nature Methods*, *14*(4), 417–419. https://doi.org/10.1038/nmeth.4197

Peeters, N. M., & Hanson, M. R. (2002). Transcript abundance supercedes editing efficiency as a factor in developmental variation of chloroplast gene expression. *RNA*, *8*(4), 497–511. https://doi.org/10.1017/S1355838202029424

Perez-Garcia, P., Serrano-Ron, L., & Moreno-Risueno, M. A. (2022). The nature of the root clock at single cell resolution: Principles of communication and similarities with plant and animal pulsatile and circadian mechanisms. *Current Opinion in Cell Biology*, *77*, 102102. https://doi.org/10.1016/j.ceb.2022.102102

Prior, K. F., O'Donnell, A. J., Rund, S. S. C., Savill, N. J., van der Veen, D. R., & Reece, S. E. (2019). Host circadian rhythms are disrupted during malaria infection in parasite genotype-specific manners. *Scientific Reports*, *9*(1). https://doi.org/10.1038/s41598-019-47191-8

R Core Team. (2021). *R: A Language and Environment for Statistical Computing*.

Rijo-Ferreira, F., Acosta-Rodriguez, V. A., Abel, J. H., Kornblum, I., Bento, I., Kilaru, G., Klerman, E. B., Mota, M. M., & Takahashi, J. S. (2020). The malaria parasite has an intrinsic clock. *Science*, *368*, 746–753. http://science.sciencemag.org/

Rijo-Ferreira, F., Takahashi, J. S., & Figueiredo, L. M. (2017). Circadian rhythms in parasites. In *PLoS Pathogens* (Vol. 13, Issue 10). Public Library of Science. https://doi.org/10.1371/journal.ppat.1006590

Rolfe, S. A., Strelkov, S. E., Links, M. G., Clarke, W. E., Robinson, S. J., Djavaheri, M., Malinowski, R., Haddadi, P., Kagale, S., Parkin, I. A. P., Taheri, A., & Borhan, M. H. (2016). The compact genome of the plant pathogen Plasmodiophora brassicae is adapted to intracellular interactions with host Brassica spp. *BMC Genomics*, *17*(1), 1–15. https://doi.org/10.1186/s12864-016-2597-2

Sanchez, S. E., & Kay, S. A. (2016). The plant circadian clock: From a simple timekeeper to a complex developmental manager. *Cold Spring Harbor Perspectives in Biology*, *8*(12), 1–16. https://doi.org/10.1101/cshperspect.a027748

Schuller, A., Kehr, J., & Ludwig-Müller, J. (2014). Laser microdissection coupled to transcriptional profiling of arabidopsis roots inoculated by plasmodiophora brassicae indicates a role for brassinosteroids in clubroot formation. *Plant and Cell Physiology*, *55*(2), 392–411. https://doi.org/10.1093/pcp/pct174

Schwelm, A., Fogelqvist, J., Knaust, A., Jülke, S., Lilja, T., Bonilla-Rosso, G., Karlsson, M., Shevchenko, A., Dhandapani, V., Choi, S. R., Kim, H. G., Park, J. Y., Lim, Y. P., Ludwig-Müller, J., & Dixelius, C. (2015). The Plasmodiophora brassicae genome reveals insights in its life cycle and ancestry of chitin synthases. *Scientific Reports*, *5*(May), 1–12. https://doi.org/10.1038/srep11153

903 Seki, M., Ohara, T., Hearn, T. J., Frank, A., Da Silva, V. C. H., Caldana, C., Webb, A. A. R., & Satake, A.
904 (2017). Adjustment of the Arabidopsis circadian oscillator by sugar signalling dictates the regulation
905 of starch metabolism. *Scientific Reports*, *7*(1), 1–11. https://doi.org/10.1038/s41598-017-08325-y

906 Shor, E., Paik, I., Kangisser, S., Green, R., & Huq, E. (2017). PHYTOCHROME INTERACTING FACTORS
907 mediate metabolic control of the circadian system in Arabidopsis. *New Phytologist*, *215*(1), 217–
908 228. https://doi.org/10.1111/nph.14579

909 Shtin, M., Dello Ioio, R., & Del Bianco, M. (2022). It's Time for a Change: The Role of Gibberellin in Root
910 Meristem Development. *Frontiers in Plant Science*, *13*(May), 1–7.
911 https://doi.org/10.3389/fpls.2022.882517

912 Siemens, J., González, M. C., Wolf, S., Hofmann, C., Greiner, S., Du, Y., Rausch, T., Roitsch, T., & Ludwig-
913 Müller, J. (2011). Extracellular invertase is involved in the regulation of clubroot disease in
914 Arabidopsis thaliana. *Molecular Plant Pathology*, *12*(3), 247–262. https://doi.org/10.1111/j.1364-
915 3703.2010.00667.x

916 Siemens, J., Keller, I., Sarx, J., Kunz, S., Schuller, A., Nagel, W., Schmülling, T., Parniske, M., & Ludwig-
917 Müller, J. (2006). Transcriptome analysis of Arabidopsis clubroots indicate a key role for cytokinins
918 in disease development. *Molecular Plant-Microbe Interactions*, *19*(5), 480–494.
919 https://doi.org/10.1094/MPMI-19-0480

920 Sierra, R., Canas-Duarte, S. J., Burki, F., Schwelm, A., Fogelqvist, J., Dixelius, C., González-García, L. N.,
921 Gile, G. H., Slamovits, C. H., Klopp, C., Restrepo, S., Arzul, I., & Pawlowski, J. (2016). Evolutionary
922 origins of rhizarian parasites. *Molecular Biology and Evolution*, *33*(4), 980–983.
923 https://doi.org/10.1093/molbev/msv340

924 Siqueira, J. A., Otoni, W. C., & Araújo, W. L. (2022). The hidden half comes into the spotlight: Peeking
925 inside the black box of root developmental phases. *Plant Communications*, *3*(1), 1–17.
926 https://doi.org/10.1016/j.xplc.2021.100246

927 Smolko, A., Jülke, S., Benade, F., Široká, J., Pěnčík, A., Vuk, T., Bauer, N., Salopek-Sondi, B., & Ludwig-
928 Müller, J. (2024). The GH3 Protein from the Clubroot Pathogen Plasmodiophora brassicae Causes
929 Hormone-Related Phenotypes in Arabidopsis thaliana. *Journal of Plant Growth Regulation*, *43*(8),
930 2715–2738. https://doi.org/10.1007/s00344-024-11300-3

931 Song, Y., Jiang, Y., Kuai, B., & Li, L. (2018). Circadian clock-associated 1 inhibits leaf senescence in
932 arabidopsis. *Frontiers in Plant Science*, *9*(March), 1–9. https://doi.org/10.3389/fpls.2018.00280

933 Stefanowicz, K., Szymanska-Chargot, M., Truman, W., Walerowski, P., Olszak, M., Augustyniak, A.,
934 Kosmala, A., Zdunek, A., & Malinowski, R. (2021). Plasmodiophora brassicae-Triggered Cell
935 Enlargement and Loss of Cellular Integrity in Root Systems Are Mediated by Pectin Demethylation.
936 *Frontiers in Plant Science*, *12*(July). https://doi.org/10.3389/fpls.2021.711838

937 Thiruvengadam, M., Shih, C. F., & Yang, C. H. (2015). Expression of An Antisense Brassica oleracea
938 GIGANTEA (BoGI) Gene in Transgenic Broccoli Causes Delayed Flowering, Leaf Senescence, and
939 Post-Harvest Yellowing Retardation. *Plant Molecular Biology Reporter*, *33*(5), 1499–1509.
940 https://doi.org/10.1007/s11105-015-0852-3

941 Tu, J., Qin, L., Karunakaran, C., Wei, Y., & Peng, G. (2024). Lignin accumulation in cell wall plays a role in
942 clubroot resistance. *Frontiers in Plant Science*, *15*(July), 1–16.
943 https://doi.org/10.3389/fpls.2024.1401265

944 Uemoto, K., Mori, F., Yamauchi, S., Kubota, A., Takahashi, N., Egashira, H., Kunimoto, Y., Araki, T.,
945 Takemiya, A., Ito, H., & Endo, M. (2023). Root PRR7 Improves the Accuracy of the Shoot Circadian
946 Clock through Nutrient Transport. *Plant and Cell Physiology*, *64*(3), 352–362.
947 https://doi.org/10.1093/pcp/pcad003

948 Vandenbussche, F., Smalle, J., Le, J., Saibo, N. J. M., De Paepe, A., Chaerle, L., Tietz, O., Smets, R.,
949 Laarhoven, L. J. J., Harren, F. J. M., Van Onckelen, H., Palme, K., Verbelen, J. P., & Van Der Straeten,
950 D. (2003). The Arabidopsis mutant alh1 illustrates a cross talk between ethylene and auxin. *Plant*
951 *Physiology*, *131*(3), 1228–1238. https://doi.org/10.1104/pp.010850

952 Walerowski, P., Gündel, A., Yahaya, N., Truman, W., Sobczak, M., Olszak, M., Rolfe, S., Borisjuk, L., &
953 Malinowski, R. (2018). Clubroot disease stimulates early steps of phloem differentiation and
954 recruits SWEET sucrose transporters within developing galls. *Plant Cell*, *30*(12), 3058–3073.
955 https://doi.org/10.1105/tpc.18.00283

956 Walter, W., Sánchez-Cabo, F., & Ricote, M. (2015). GOplot: An R package for visually combining
957 expression data with functional analysis. *Bioinformatics*, *31*(17), 2912–2914.
958 https://doi.org/10.1093/bioinformatics/btv300

959 Walters, D. R., & McRoberts, N. (2006). Plants and biotrophs: a pivotal role for cytokinins? *Trends in Plant*
960 *Science*, *11*(12), 581–586. https://doi.org/10.1016/j.tplants.2006.10.003

961 Wang, J., Xu, G., Ning, Y., Wang, X., & Wang, G. L. (2022). Mitochondrial functions in plant immunity. In
962 *Trends in Plant Science* (Vol. 27, Issue 10, pp. 1063–1076). Elsevier Ltd.
963 https://doi.org/10.1016/j.tplants.2022.04.007

964 Wang, S., Steed, G., & Webb, A. A. R. (2022). Circadian entrainment in Arabidopsis. *Plant Physiology*,
965 *190*(2), 981–993. https://doi.org/10.1093/plphys/kiac204

966 Wang, X., An, Y., Xu, P., & Xiao, J. (2021). Functioning of PPR Proteins in Organelle RNA Metabolism and
967 Chloroplast Biogenesis. *Frontiers in Plant Science*, *12*(February), 1–8.
968 https://doi.org/10.3389/fpls.2021.627501

969 Wang, Y., & Tan, B. C. (2025). Pentatricopeptide repeat proteins in plants: Cellular functions, action
970 mechanisms, and potential applications. In *Plant Communications* (Vol. 6, Issue 2). Cell Press.
971 https://doi.org/10.1016/j.xplc.2024.101203

972 Wei, X., Zhang, Y., Zhao, Y., Xie, Z., Hossain, M. R., Yang, S., Shi, G., Lv, Y., Wang, Z., Tian, B., Su, H., Wei,
973 F., Zhang, X., & Yuan, Y. (2021). Root Transcriptome and Metabolome Profiling Reveal Key
974 Phytohormone-Related Genes and Pathways Involved Clubroot Resistance in Brassica rapa L.
975 *Frontiers in Plant Science*, *12*(December), 1–17. https://doi.org/10.3389/fpls.2021.759623

976 Wickham, H. (2010). ggplot2: Elegant Graphics for Data Analysis. *Journal of Statistical Software*, *1*(1),
977 128–129. https://doi.org/10.1002/wics.10

978 Wu, T., Hu, E., Xu, S., Chen, M., Guo, P., Dai, Z., Feng, T., Zhou, L., Tang, W., Zhan, L., Fu, X., Liu, S., Bo, X.,
979 & Yu, G. (2021). clusterProfiler 4.0: A universal enrichment tool for interpreting omics data.
980 *Innovation*, *2*(3), 100141. https://doi.org/10.1016/j.xinn.2021.100141

981 Yang, Y., Fan, G., Zhao, Y., Wen, Q., Wu, P., Meng, Y., & Shan, W. (2020). Cytidine-to-uridine RNA editing
982 factor NbMORF8 negatively regulates plant immunity to phytophthora pathogens. *Plant Physiology*,
983 *184*(4), 2182–2198. https://doi.org/10.1104/pp.20.00458

984 Yang, Y., Zhao, Y., Zhang, Y., Niu, L., Li, W., Lu, W., Li, J., Schäfer, P., Meng, Y., & Shan, W. (2022). A
985 mitochondrial RNA processing protein mediates plant immunity to a broad spectrum of pathogens
986 by modulating the mitochondrial oxidative burst. *Plant Cell*, *34*(6), 2343–2363.
987 https://doi.org/10.1093/plcell/koac082

988 Yazdanbakhsh, N., & Fisahn, J. (2010). Analysis of Arabidopsis thaliana root growth kinetics with high
989 temporal and spatial resolution. *Annals of Botany*, *105*(5), 783–791.
990 https://doi.org/10.1093/aob/mcq048

991 Yazdanbakhsh, N., Sulpice, R., Graf, A., Stitt, M., & Fisahn, J. (2011). Circadian control of root elongation
992 and C partitioning in Arabidopsis thaliana. *Plant, Cell and Environment*, *34*(6), 877–894.
993 https://doi.org/10.1111/j.1365-3040.2011.02286.x

994 Zheng, X. Y., Zhou, M., Yoo, H., Pruneda-Paz, J. L., Spivey, N. W., Kay, S. A., & Dong, X. (2015). Spatial and
995 temporal regulation of biosynthesis of the plant immune signal salicylic acid. *Proceedings of the*
996 *National Academy of Sciences of the United States of America*, *112*(30), 9166–9173.
997 https://doi.org/10.1073/pnas.1511182112

998 Zhu, J. Y., Oh, E., Wang, T., & Wang, Z. Y. (2016). TOC1-PIF4 interaction mediates the circadian gating of
999 thermoresponsive growth in Arabidopsis. *Nature Communications*, *7*, 1–10.
1000 https://doi.org/10.1038/ncomms13692

1001

Supporting information

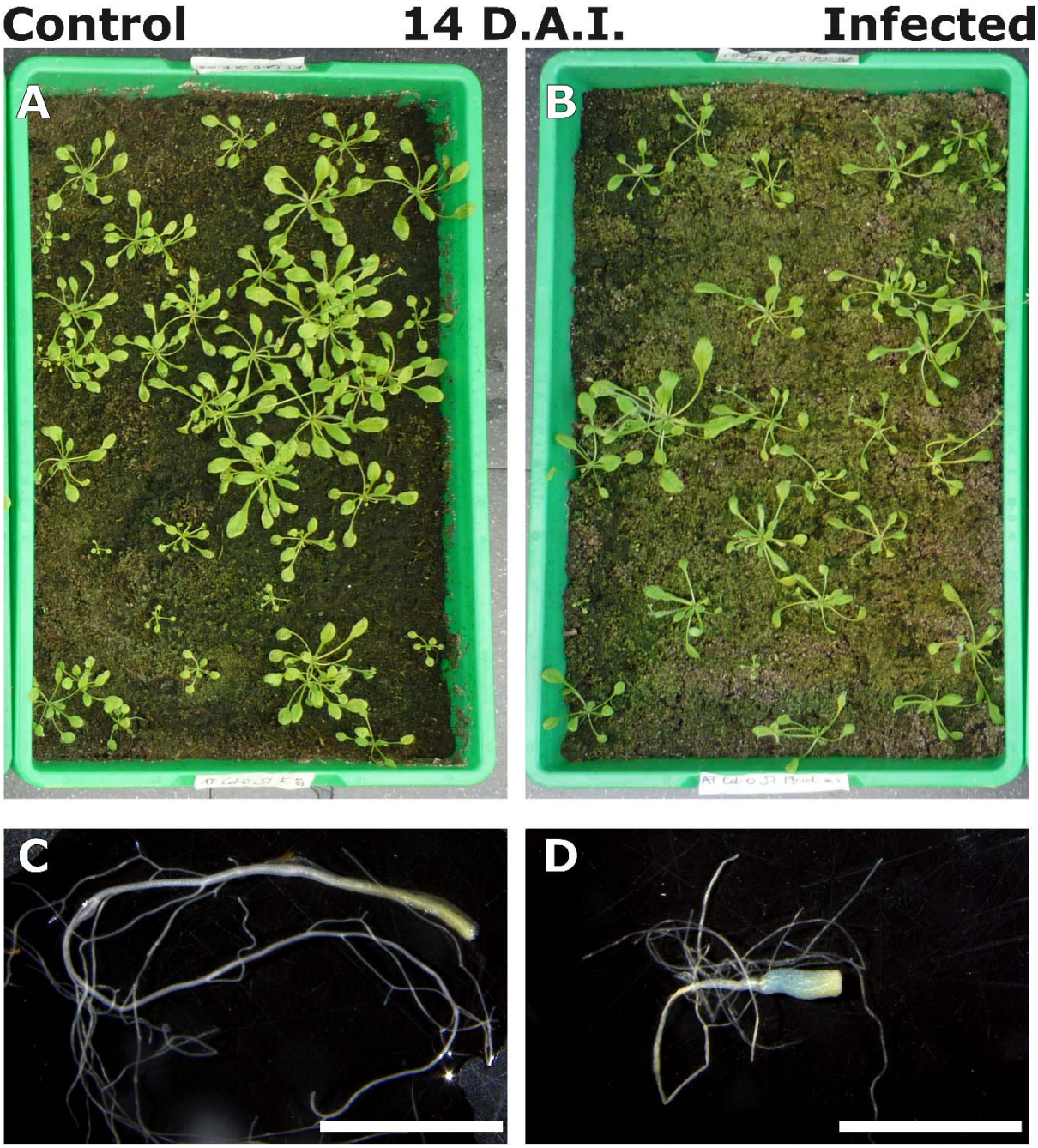

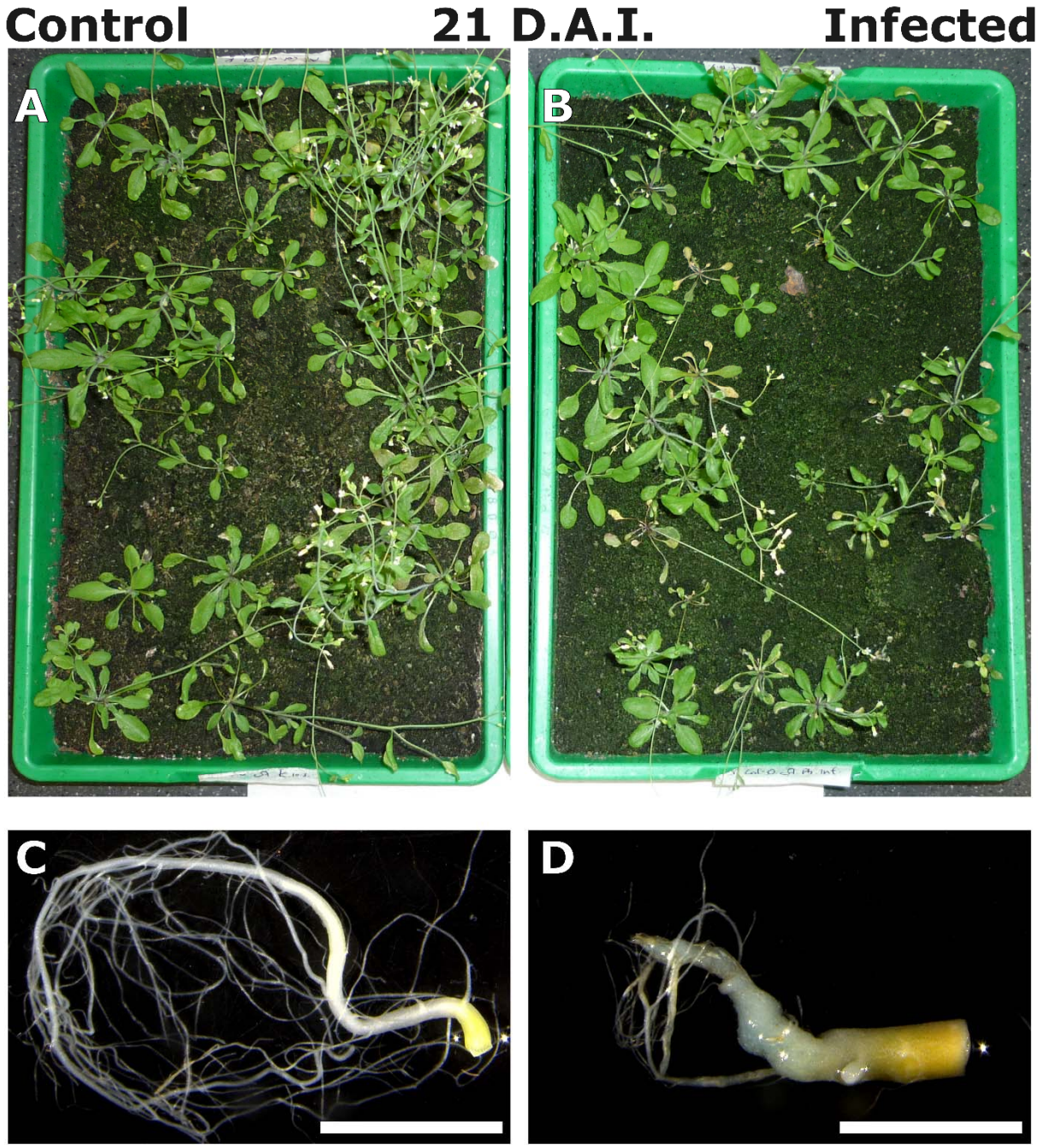

Additional File 1 Phenotypical traits of rosettes (A and B) and root samples (C and D) for specimen of healthy and infected A. thaliana Col-0 harvested at 14 d.a.i. (top figure plate) and 21 d.a.i. (bottom figure plate). Scale bars in C and D = 5 mm.

Additional File 2 Detailed overview of the samples sequenced in this study

Condition	Age (days after infection)	Hours after artificial dawn	Replicate	Raw reads

			code	
Control	14	5 hr 50' (day)	127925	41193025
		5 hr 50' (day)	127935	50545664
		5 hr 50' (day)	127936	35205326
		10 hr 40' (day)	127906	56725609
		10 hr 40' (day)	127912	54273366
		10 hr 40' (day)	127918	38720139
		15 hr 30' (night)	127926	41309013
		15 hr 30' (night)	127931	55027843
		15 hr 30' (night)	127937	38004169
		19 hr 20' (night)	127907	39958547
		19 hr 20' (night)	127913	37101449
		19 hr 20' (night)	127919	40693049
Infected	14	5 hr 50' (day)	127964	48508205
		5 hr 50' (day)	127970	41810661
		5 hr 50' (day)	127976	54739923
		10 hr 40' (day)	127946	42594195
		10 hr 40' (day)	127952	41155738
		10 hr 40' (day)	127958	58101982
		15 hr 30' (night)	127965	43247574
		15 hr 30' (night)	127971	46509846
		15 hr 30' (night)	127977	57602784
		19 hr 20' (night)	127947	40263406
		19 hr 20' (night)	127953	41398461
		19 hr 20' (night)	127959	50627500
Control	21	5 hr 50' (day)	127908	52533389
		5 hr 50' (day)	127914	36118824
		5 hr 50' (day)	127941	64871718
		10 hr 40' (day)	127928	41179331
		10 hr 40' (day)	127933	45662748
		10 hr 40' (day)	127939	54002775
		15 hr 30' (night)	127909	43278660
		15 hr 30' (night)	127915	43201375
		15 hr 30' (night)	127920	42466381
		19 hr 20' (night)	127929	43287455
		19 hr 20' (night)	127934	46270564
		19 hr 20' (night)	127940	53657896
Infected	21	5 hr 50' (day)	127948	59286277
		5 hr 50' (day)	127954	62740880
		5 hr 50' (day)	127960	46195940
		10 hr 40' (day)	127967	48074903
		10 hr 40' (day)	127973	61491275
		10 hr 40' (day)	127979	62580301

15 hr 30' (night)	127949	55537283
15 hr 30' (night)	127955	65514599
15 hr 30' (night)	127961	54889653
19 hr 20' (night)	127968	85469436
19 hr 20' (night)	127974	71731948
19 hr 20' (night)	127980	58536488

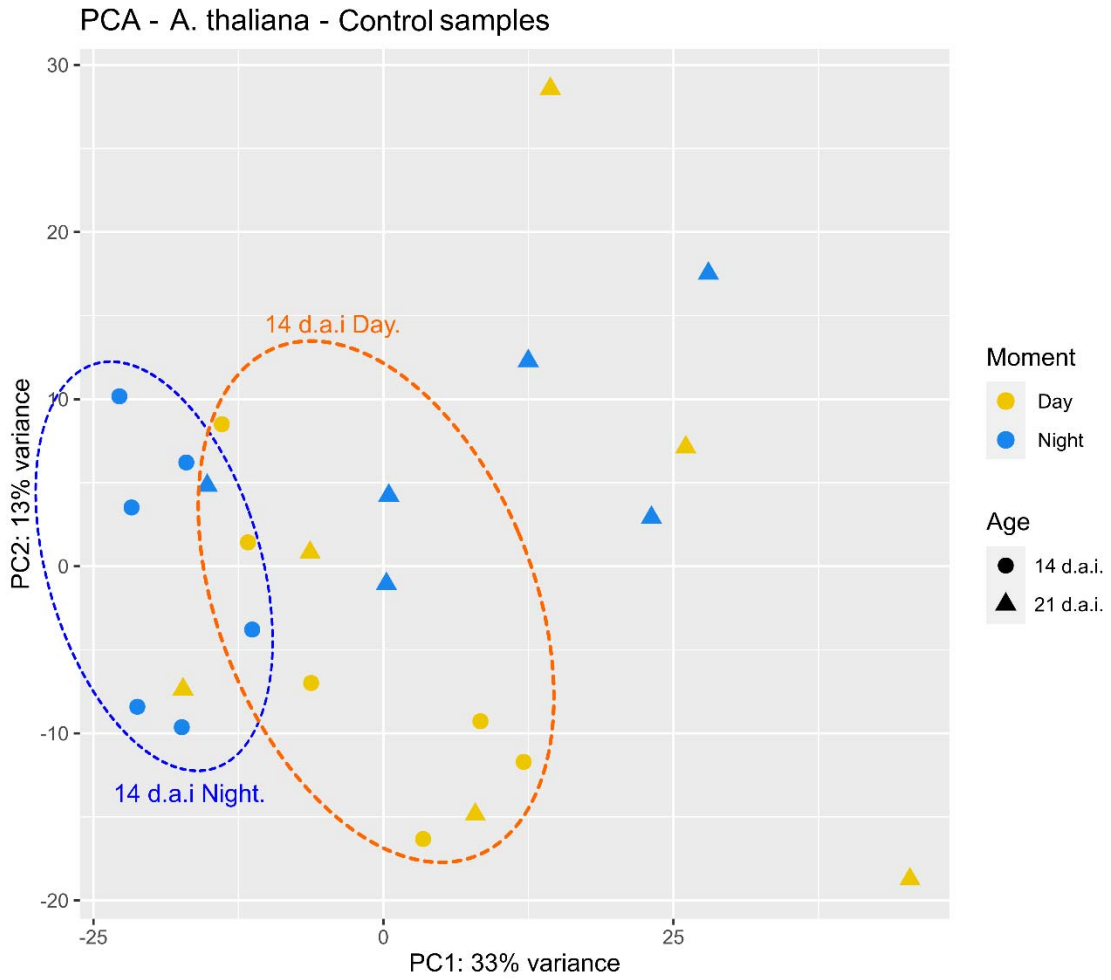

1021

1022 *Additional File 3 PCA on control A. thaliana plants, showing the decreased influence of the temporal factor (i.e., day and night)*
1023 *on the overall gene expression levels with the ageing of the plants.*

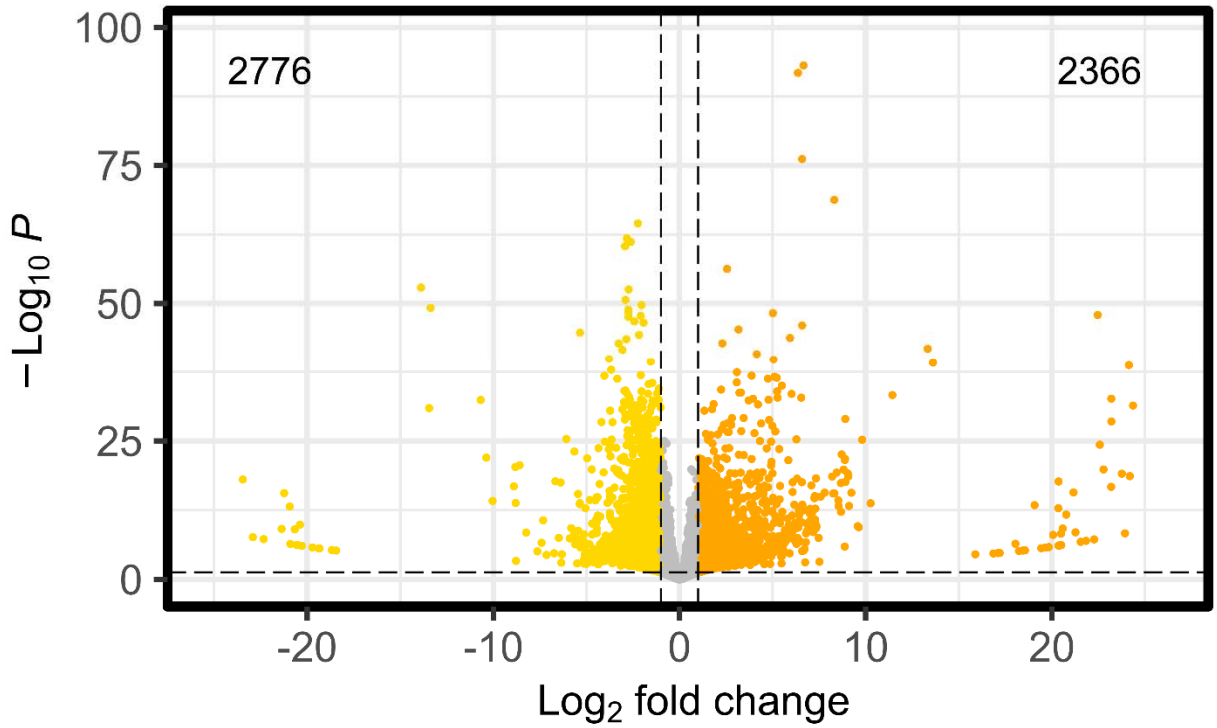

1024

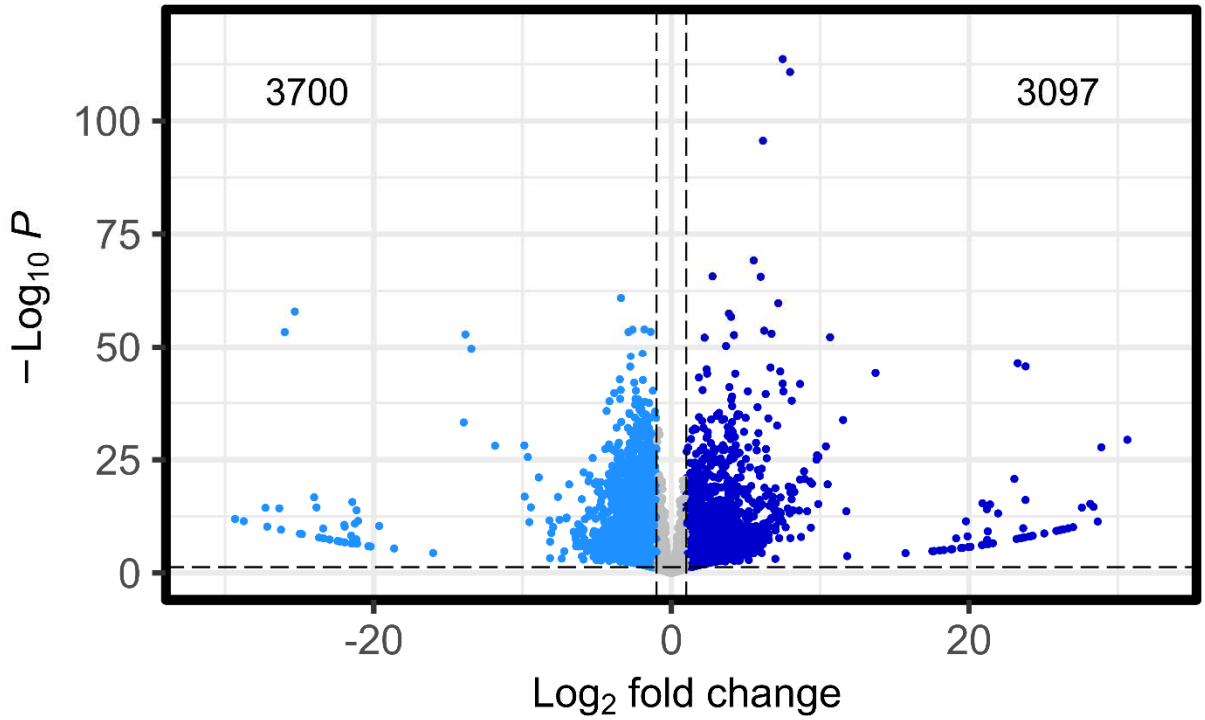

1025

1026 *Additional File 4 Volcano plot showing the number of DEGs in the day (top figure) and night (bottom figure) in infected A.*
1027 *thaliana plants 14 DAI*

1028

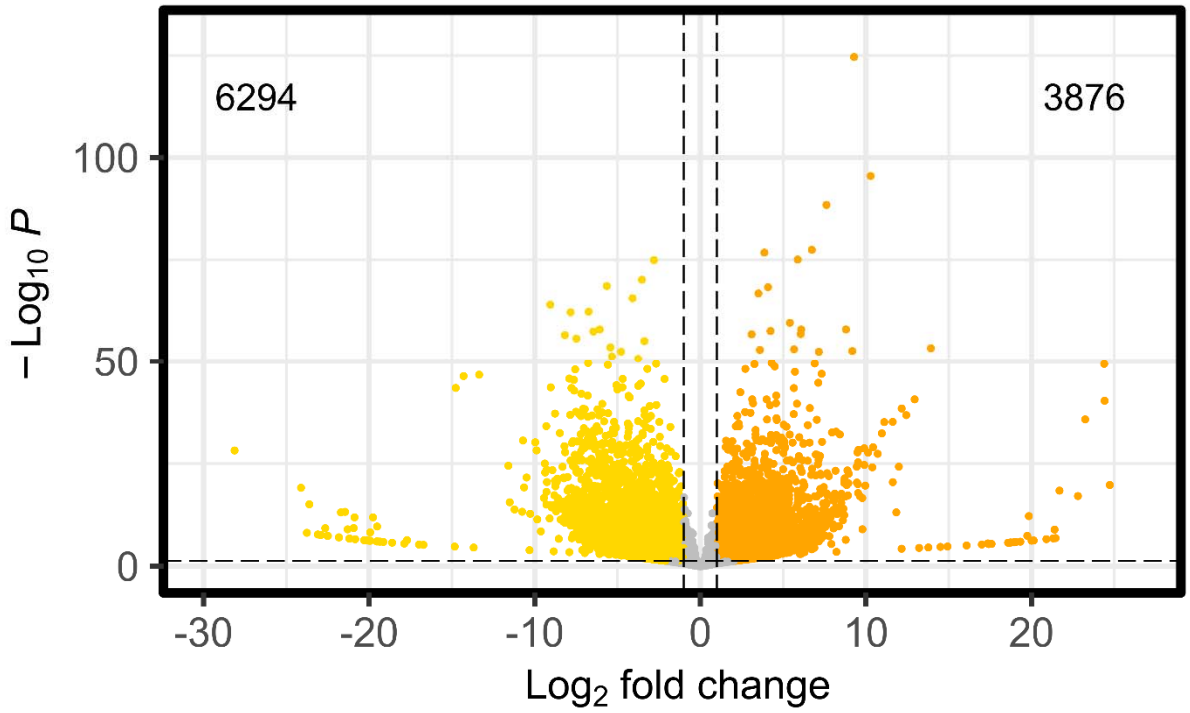

1029

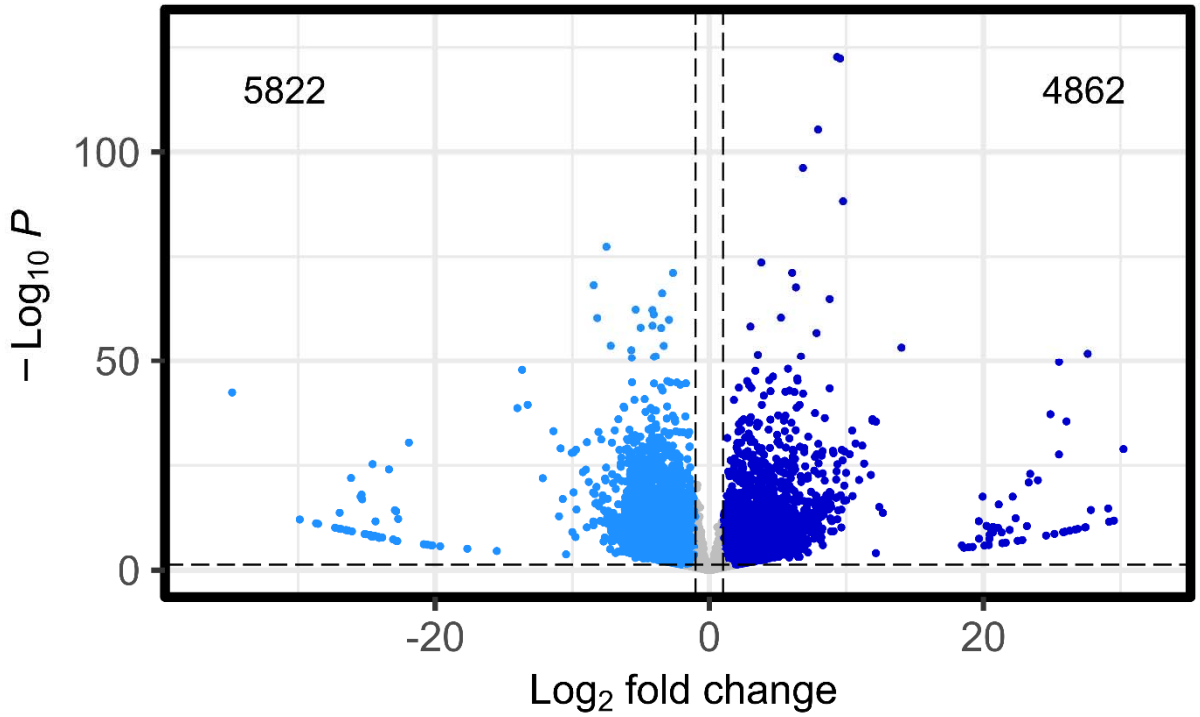

1030

1031 *Additional File 5 Volcano plot showing the number of DEGs in the day (top figure) and night (bottom figure) in infected A.*
1032 *thaliana plants 21 DAI*

1033

1034

1035 *Additional File 6 All GO categories enriched in DEGs in A. thaliana roots 14 DAI infected by P. brassicae as in Fig 3. GO categories*
1036 *are organised by decreasing -log10 adjusted p-value (i.e., top to bottom in the relative figure).*

GO term categories affected by *P.brassicae* infection in *A. thaliana* 14 d.a.i.									
Day					Night				
Upregulated									
ID	term	count	adj_pval	zscore	ID	term	count	adj_pval	zscore
GO:0009636	response to toxic substance	55	8,92	3,64	GO:0009636	response to toxic substance	68	11,73	3,40
GO:0046906	tetrapyrrole binding	89	7,47	1,38	GO:0009451	RNA modification	101	7,86	7,06
GO:0048646	anatomical structure formation involved in morphogenesis	68	5,68	1,21	GO:0140359	ABC-type transporter activity	41	6,98	0,47
GO:0008299	isoprenoid biosynthetic process	54	4,74	0,27	GO:0090332	stomatal closure	26	5,69	0,39
GO:0048580	regulation of post-embryonic development	91	4,41	0,31	GO:0000302	response to reactive oxygen species	50	5,36	0,28
GO:0046148	pigment biosynthetic process	52	4,38	1,94	GO:0002213	defense response to insect	32	4,97	1,06
GO:0038023	signaling receptor activity	36	4,31	0,67	GO:0048580	regulation of post-embryonic development	108	4,70	0,38
GO:0048046	apoplast	70	4,22	1,20	GO:0009739	response to gibberellin	40	4,41	0,32
GO:0010287	plastoglobule	21	3,75	2,40	GO:0048544	recognition of pollen	20	3,82	3,13
GO:0009767	photosynthetic electron transport chain	19	3,41	3,44	GO:0009991	response to extracellular stimulus	79	3,60	0,11
GO:0042651	thylakoid membrane	73	3,14	5,97	GO:0045165	cell fate commitment	30	2,96	0,73
GO:0016829	lyase activity	65	3,06	0,12	GO:0099503	secretory vesicle	46	2,90	0,59
GO:0009739	response to gibberellin	31	2,94	1,26	GO:0071214	cellular response to abiotic stimulus	63	2,81	0,13
GO:0009644	response to high light intensity	19	2,87	1,15	GO:0007166	cell surface receptor signaling pathway	19	2,70	0,69
GO:0015267	channel activity	41	2,86	0,47	GO:2000377	regulation of reactive oxygen species metabolic process	21	2,63	1,53
GO:0102483	scopolin beta-glucosidase activity	14	2,39	0,53	GO:0009723	response to ethylene	60	2,45	0,26
GO:0010168	ER body	7	2,35	2,65	GO:1902679	negative regulation of RNA biosynthetic process	53	2,45	0,41
GO:0016054	organic acid catabolic process	35	2,09	0,85	GO:0008171	O-methyltransferase activity	16	2,38	0,50
GO:2000377	regulation of reactive oxygen species metabolic process	17	2,02	1,21	GO:0048825	cotyledon development	18	2,32	1,41
GO:0048544	recognition of pollen	14	1,96	0,53	GO:0000712	resolution of meiotic recombination intermediates	7	2,21	2,65
GO:0000373	Group II intron splicing	9	1,82	0,33	GO:0042440	pigment metabolic process	82	2,01	0,66
GO:0009630	gravitropism	21	1,66	0,65	GO:0008283	cell population proliferation	27	1,90	0,96
GO:0008283	cell population proliferation	22	1,51	0,43	GO:0048235	pollen sperm cell differentiation	12	1,87	0,58
GO:1900865	chloroplast RNA modification	6	1,45	1,63	GO:0000079	regulation of cyclin-dependent protein serine/threonine	15	1,84	0,26

						kinase activity			
GO:0006638	neutral lipid metabolic process	10	1,41	0,63	GO:0042793	plastid transcription	7	1,84	1,89
					GO:0002832	negative regulation of response to biotic stimulus	15	1,78	0,77
					GO:0010114	response to red light	25	1,64	0,20
					GO:0010090	trichome morphogenesis	19	1,63	0,23
					GO:0019432	triglyceride biosynthetic process	9	1,47	0,33
					GO:1901681	sulfur compound binding	11	1,40	0,30
Zero z-score									
ID	**term**	**count**	**adj_pval**	**zscore**	**ID**	**term**	**count**	**adj_pval**	**zscore**
GO:0002238	response to molecule of fungal origin	10	3,43	0,00	GO:0008299	isoprenoid biosynthetic process	74	8,81	0,00
					GO:0048437	floral organ development	72	4,62	0,00
					GO:1901698	response to nitrogen compound	64	3,43	0,00
					GO:0009608	response to symbiont	6	1,75	0,00
					GO:0009629	response to gravity	26	1,66	0,00
Downregulated									
ID	**term**	**count**	**adj_pval**	**zscore**	**ID**	**term**	**count**	**adj_pval**	**zscore**
GO:0071456	cellular response to hypoxia	86	18,78	-3,23	GO:0044262	cellular carbohydrate metabolic process	144	17,31	-5,33
GO:0044262	cellular carbohydrate metabolic process	125	17,57	-4,74	GO:0003953	NAD+ nucleosidase activity	27	16,14	-4,81
GO:0044550	secondary metabolite biosynthetic process	107	14,08	-3,77	GO:0009698	phenylpropanoid metabolic process	64	14,42	-3,25
GO:0003953	NAD+ nucleosidase activity	24	14,04	-3,27	GO:0036294	cellular response to decreased oxygen levels	87	13,71	-3,11
GO:0009751	response to salicylic acid	107	11,64	-4,54	GO:0016798	hydrolase activity acting on glycosyl bonds	127	11,94	-5,06
GO:0012501	programmed cell death	59	9,99	-2,21	GO:0020037	heme binding	104	9,74	-0,98
GO:0048584	positive regulation of response to stimulus	72	7,78	-1,89	GO:0009751	response to salicylic acid	117	9,70	-2,68
GO:0042537	benzene-containing compound metabolic process	29	7,18	-2,79	GO:0045229	external encapsulating structure organization	107	9,36	-3,96
GO:0042802	identical protein binding	89	6,82	-0,74	GO:0016143	S-glycoside metabolic process	82	9,34	-1,77
GO:0048437	floral organ development	69	6,71	-0,12	GO:0048646	anatomical structure formation involved in morphogenesis	87	8,42	-1,61
GO:0000302	response to reactive oxygen species	47	6,58	-0,44	GO:0048584	positive regulation of response to stimulus	84	8,32	-0,44
GO:0062012	regulation of small molecule metabolic process	54	6,54	-4,08	GO:0010087	phloem or xylem histogenesis	55	7,08	-4,45
GO:0045229	external encapsulating structure organization	81	5,53	-3,22	GO:2000652	regulation of secondary cell wall biogenesis	28	6,87	-4,54
GO:0090332	stomatal closure	23	5,38	-1,46	GO:0042537	benzene-containing compound metabolic process	31	6,56	-3,05
GO:19	regulation of cell wall	25	5,14	-4,60	GO:00	organic acid transport	46	5,92	-1,18

03338	organization or biogenesis				15849				
GO:0009743	response to carbohydrate	48	4,95	-0,87	GO:0010150	leaf senescence	83	5,86	-0,77
GO:0016747	acyltransferase activity transferring groups other than amino-acyl groups	69	4,63	-0,60	GO:0010648	negative regulation of cell communication	41	5,85	-0,78
GO:0048585	negative regulation of response to stimulus	56	4,49	-0,80	GO:0006811	monoatomic ion transport	94	5,78	-0,83
GO:0010087	phloem or xylem histogenesis	41	4,16	-3,90	GO:0015698	inorganic anion transport	40	5,54	-1,58
GO:0015698	inorganic anion transport	32	4,09	-0,71	GO:0010143	cutin biosynthetic process	16	5,41	-0,50
GO:0009733	response to auxin	83	3,77	-0,99	GO:0008219	cell death	68	5,30	-2,43
GO:0010150	leaf senescence	64	3,75	-0,75	GO:0000981	DNA-binding transcription factor activity RNA polymerase II-specific	79	5,30	-0,56
GO:0046777	protein autophosphorylation	40	3,70	-2,85	GO:0007623	circadian rhythm	49	4,99	-0,43
GO:0042594	response to starvation	48	3,64	-0,29	GO:0090627	plant epidermal cell differentiation	62	4,92	-2,29
GO:0140359	ABC-type transporter activity	29	3,49	-0,56	GO:0071365	cellular response to auxin stimulus	42	4,84	-0,31
GO:0015849	organic acid transport	34	3,43	-0,34	GO:0042802	identical protein binding	94	4,33	-0,62
GO:0006816	calcium ion transport	23	3,38	-1,46	GO:0009735	response to cytokinin	39	3,62	-1,12
GO:0048235	pollen sperm cell differentiation	13	3,02	-0,28	GO:0009308	amine metabolic process	43	3,48	-2,29
GO:0070417	cellular response to cold	13	3,02	-0,28	GO:0043621	protein self-association	35	3,32	-0,51
GO:0043621	protein self-association	29	2,79	-0,56	GO:0034285	response to disaccharide	25	3,22	-1,80
GO:0006631	fatty acid metabolic process	61	2,77	-0,38	GO:0019899	enzyme binding	81	3,01	-2,33
GO:0009308	amine metabolic process	35	2,76	-2,87	GO:0022603	regulation of anatomical structure morphogenesis	50	2,84	-1,70
GO:0009624	response to nematode	22	2,76	-1,28	GO:0046777	protein autophosphorylation	43	2,83	-0,15
GO:1901698	response to nitrogen compound	52	2,72	-0,28	GO:0009741	response to brassinosteroid	34	2,65	-2,74
GO:0042887	amide transmembrane transporter activity	18	2,64	-1,41	GO:0009705	plant-type vacuole membrane	36	2,58	-1,33
GO:0048767	root hair elongation	21	2,46	-1,53	GO:0015295	solute:proton symporter activity	13	2,57	-0,83
GO:0009408	response to heat	70	2,46	-0,96	GO:0006880	intracellular sequestering of iron ion	8	2,47	-0,71
GO:0019900	kinase binding	29	2,43	-3,53	GO:0009826	unidimensional cell growth	96	2,45	-2,04
GO:0010073	meristem maintenance	51	2,41	-0,42	GO:0048046	apoplast	72	2,44	-1,18
GO:0009625	response to insect	13	2,38	-0,28	GO:0009624	response to nematode	24	2,42	-0,82
GO:0000981	DNA-binding transcription factor activity RNA polymerase II-specific	56	2,32	-0,53	GO:0006833	water transport	14	2,34	-1,07
GO:0051644	plastid localization	9	2,27	-0,33	GO:0008236	serine-type peptidase activity	43	2,33	-1,98
GO:00	nucleoside	11	2,24	-2,11	GO:00	meristem maintenance	59	2,26	-0,13

05337	transmembrane transporter activity				10073				
GO:0042578	phosphoric ester hydrolase activity	66	2,24	-2,95	GO:0051119	sugar transmembrane transporter activity	19	2,18	-1,61
GO:0071215	cellular response to abscisic acid stimulus	59	2,19	-3,78	GO:0042886	amide transport	15	2,18	-1,29
GO:0007389	pattern specification process	60	2,11	-1,03	GO:0010038	response to metal ion	51	2,05	-2,66
GO:0009705	plant-type vacuole membrane	29	2,06	-1,30	GO:0008374	O-acyltransferase activity	30	2,02	-2,92
GO:0009531	secondary cell wall	9	2,06	-3,00	GO:0009411	response to UV	31	2,00	-0,90
GO:0005507	copper ion binding	37	2,01	-0,16	GO:0030570	pectate lyase activity	10	1,96	-0,63
GO:0055062	phosphate ion homeostasis	9	1,91	-1,00	GO:0070417	cellular response to cold	12	1,87	-0,58
GO:0009269	response to desiccation	9	1,91	-1,67	GO:0035556	intracellular signal transduction	90	1,87	-1,26
GO:0009826	unidimensional cell growth	77	1,82	-1,71	GO:0010214	seed coat development	17	1,87	-1,70
GO:0004620	phospholipase activity	15	1,76	-1,81	GO:0051049	regulation of transport	30	1,85	-1,46
GO:0071214	cellular response to abiotic stimulus	48	1,64	-0,29	GO:0050660	flavin adenine dinucleotide binding	37	1,84	-0,82
GO:0009735	response to cytokinin	27	1,58	-0,96	GO:0004551	dinucleotide phosphatase activity	6	1,84	-1,63
GO:0008171	O-methyltransferase activity	12	1,53	-0,58	GO:0009615	response to virus	25	1,83	-1,00
GO:0030145	manganese ion binding	13	1,52	-3,05	GO:0006631	fatty acid metabolic process	65	1,67	-1,86
GO:0050660	flavin adenine dinucleotide binding	30	1,51	-0,37	GO:0009850	auxin metabolic process	19	1,63	-0,23
GO:0040034	regulation of development heterochronic	13	1,47	-0,28	GO:0009408	response to heat	77	1,63	-1,48
GO:0045926	negative regulation of growth	10	1,47	-0,63	GO:0016829	lyase activity	68	1,60	-0,73
GO:0071367	cellular response to brassinosteroid stimulus	18	1,45	-2,36	GO:0051923	sulfation	7	1,55	-2,65
GO:0016307	phosphatidylinositol phosphate kinase activity	6	1,43	-0,82	GO:0030145	manganese ion binding	15	1,54	-3,36
GO:0015081	sodium ion transmembrane transporter activity	11	1,32	-1,51	GO:0007010	cytoskeleton organization	65	1,49	-3,35
					GO:0009269	response to desiccation	9	1,47	-1,67
					GO:0090158	endoplasmic reticulum membrane organization	6	1,42	-1,63
					GO:0015851	nucleobase transport	9	1,38	-1,00
					GO:0009631	cold acclimation	15	1,31	-2,32

1042

1043 *Additional File 7 All GO categories enriched in DEGs in A. thaliana roots 21 DAI infected by P. brassicae as in Fig 3. GO categories*
1044 *are organised by decreasing -log10 adjusted p-value (i.e., top to bottom in the relative figure).*

GO term categories affected by *P.brassicae* infection in *A. thaliana* 21 d.a.i.									
Day					Night				
Upregulated									
ID	term	count	adj_pval	zscore	ID	term	count	adj_pval	zscore
GO:0015979	photosynthesis	123	14,82	8,75	GO:0015979	photosynthesis	132	16,94	9,05
GO:0009657	plastid organization	121	11,02	5,36	GO:0009991	response to extracellular stimulus	148	14,73	1,97
GO:0016054	organic acid catabolic process	76	8,94	0,92	GO:0009657	plastid organization	131	12,99	6,55
GO:0046148	pigment biosynthetic process	91	8,43	3,25	GO:0003953	NAD+ nucleosidase activity	27	11,87	0,19
GO:0009646	response to absence of light	33	8,32	0,87	GO:0000302	response to reactive oxygen species	81	11,34	0,56
GO:0007623	circadian rhythm	68	6,98	0,97	GO:0042802	identical protein binding	151	9,49	0,08
GO:0009639	response to red or far red light	134	5,25	0,69	GO:0044282	small molecule catabolic process	99	9,20	0,90
GO:0002213	defense response to insect	37	3,95	0,49	GO:0009642	response to light intensity	143	9,17	5,44
GO:0005777	peroxisome	94	2,63	0,41	GO:0015995	chlorophyll biosynthetic process	51	8,01	4,90
GO:0000373	Group II intron splicing	13	2,17	1,39	GO:0071214	cellular response to abiotic stimulus	107	7,63	1,45
GO:0007166	cell surface receptor signaling pathway	21	1,81	2,40	GO:0007623	circadian rhythm	72	7,53	2,59
GO:0006641	triglyceride metabolic process	14	1,79	0,53	GO:0009743	response to carbohydrate	81	7,52	1,00
GO:1901361	organic cyclic compound catabolic process	90	1,55	0,84	GO:0010150	leaf senescence	115	6,56	1,40
GO:0015749	monosaccharide transmembrane transport	12	1,49	1,15	GO:0051093	negative regulation of developmental process	73	5,26	0,35
GO:0005315	inorganic phosphate transmembrane transporter activity	9	1,35	1,00	GO:0071949	FAD binding	37	4,80	1,81
					GO:0043621	protein self-association	50	4,58	0,28
					GO:0015144	carbohydrate transmembrane transporter activity	39	4,41	0,48
					GO:0051253	negative regulation of RNA metabolic	81	3,19	0,56

						process			
					GO:0002213	defense response to insect	36	3,10	0,33
					GO:0008271	secondary active sulfate transmembrane transporter activity	9	3,00	0,33
					GO:0010014	meristem initiation	21	2,49	0,22
					GO:0022411	cellular component disassembly	40	2,33	0,63
					GO:0009704	de-etiolation	10	2,29	0,63
					GO:0040034	regulation of development heterochronic	22	2,28	0,43
					GO:0009739	response to gibberellin	45	2,28	0,45
					GO:0000373	Group II intron splicing	13	2,01	1,39
					GO:1900865	chloroplast RNA modification	9	1,92	2,33
					GO:0010181	FMN binding	13	1,57	0,83
					GO:0045454	cell redox homeostasis	16	1,48	2,50
					GO:0031406	carboxylic acid binding	37	1,33	0,82
					GO:0019432	triglyceride biosynthetic process	11	1,32	0,90
Zero z-score									
ID	**term**	**count**	**adj_pval**	**zscore**	**ID**	**term**	**count**	**adj_pval**	**zscore**
GO:0080027	response to herbivore	18	6,49	0	GO:0009636	response to toxic substance	94	15,27	0
GO:1901699	cellular response to nitrogen compound	32	4,90	0	GO:0010118	stomatal movement	78	9,44	0
GO:0009624	response to nematode	36	4,40	0					
GO:0004033	aldo-keto reductase (NADP) activity	12	2,49	0					
Downregulated									
ID	**term**	**count**	**adj_pval**	**zscore**	**ID**	**term**	**count**	**adj_pval**	**zscore**
GO:0044262	cellular carbohydrate metabolic process	196	23,13	-6,00	GO:0044262	cellular carbohydrate metabolic process	208	25,39	-5,82
GO:0009698	phenylpropanoid metabolic process	84	18,71	-4,80	GO:0044550	secondary metabolite biosynthetic process	171	17,41	-8,34

GO:0009636	response to toxic substance	94	16,84	-1,24	GO:0045229	external encapsulating structure organization	156	13,46	-7,37
GO:0003953	NAD+ nucleosidase activity	29	15,42	-0,93	GO:0046906	tetrapyrrole binding	158	12,94	-1,91
GO:0046906	tetrapyrrole binding	158	15,42	-1,75	GO:0098660	inorganic ion transmembrane transport	107	12,43	-1,64
GO:0016143	S-glycoside metabolic process	117	14,45	-6,19	GO:0006721	terpenoid metabolic process	120	12,11	-0,55
GO:0036294	cellular response to decreased oxygen levels	109	14,30	-3,93	GO:0036294	cellular response to decreased oxygen levels	107	11,74	-3,96
GO:0009991	response to extracellular stimulus	139	13,31	-0,93	GO:0090698	post-embryonic plant morphogenesis	99	11,65	-1,51
GO:0045229	external encapsulating structure organization	148	12,76	-7,07	GO:0140359	ABC-type transporter activity	60	11,13	-1,29
GO:0009751	response to salicylic acid	159	12,21	-5,63	GO:0009751	response to salicylic acid	162	11,09	-5,34
GO:0048046	apoplast	126	11,47	-1,07	GO:0006631	fatty acid metabolic process	132	11,01	-1,04
GO:0000302	response to reactive oxygen species	76	10,23	-0,46	GO:1901615	organic hydroxy compound metabolic process	158	10,82	-2,23
GO:0098660	inorganic ion transmembrane transport	94	8,68	-1,24	GO:0048046	apoplast	127	10,03	-0,44
GO:0010016	shoot system morphogenesis	104	8,66	-3,14	GO:0090627	plant epidermal cell differentiation	93	7,81	-4,87
GO:0006721	terpenoid metabolic process	106	8,62	-2,33	GO:0009966	regulation of signal transduction	155	7,60	-4,10
GO:0042537	benzene-containing compound metabolic process	41	8,59	-2,97	GO:0042446	hormone biosynthetic process	40	7,56	-3,48
GO:0006631	fatty acid metabolic process	119	8,38	-1,19	GO:0006955	immune response	114	7,50	-0,75
GO:0090696	post-embryonic plant organ development	83	7,98	-1,43	GO:0015849	organic acid transport	63	7,27	-1,64
GO:0016798	hydrolase activity acting on glycosyl bonds	150	7,89	-5,88	GO:0016829	lyase activity	123	6,77	-3,70
GO:0090627	plant epidermal cell differentiation	89	7,64	-6,04	GO:0016746	acyltransferase activity	127	6,66	-2,40
GO:0006955	immune response	110	7,60	-3,05	GO:0009624	response to nematode	42	6,55	-0,31
GO:0016747	acyltransferase activity transferring groups other than amino-acyl groups	116	7,43	-2,04	GO:0009225	nucleotide-sugar metabolic process	30	6,10	-3,65
GO:0010817	regulation of hormone levels	107	7,40	-5,32	GO:2000280	regulation of root development	39	5,74	-2,08

GO:0015849	organic acid transport	61	7,34	-2,94	GO:0010038	response to metal ion	87	5,69	-2,47
GO:0140359	ABC-type transporter activity	51	7,24	-1,82	GO:0010143	cutin biosynthetic process	19	5,47	-1,61
GO:0016682	oxidoreductase activity acting on diphenols and related substances as donors oxygen as acceptor	21	7,08	-3,71	GO:0015267	channel activity	74	5,30	-1,86
GO:1901615	organic hydroxy compound metabolic process	138	6,97	-2,04	GO:0009741	response to brassinosteroid	54	5,25	-2,72
GO:0010118	stomatal movement	69	6,91	-1,81	GO:0009733	response to auxin	144	5,24	-2,17
GO:0010087	phloem or xylem histogenesis	68	6,77	-5,82	GO:0048226	Casparian strip	13	4,87	-3,61
GO:0042802	identical protein binding	134	6,56	-1,21	GO:0022626	cytosolic ribosome	106	4,85	-6,60
GO:0009741	response to brassinosteroid	55	6,42	-3,10	GO:0005856	cytoskeleton	124	4,80	-5,75
GO:0048226	Casparian strip	14	6,39	-3,74	GO:0035556	intracellular signal transduction	146	4,40	-1,99
GO:0022626	cytosolic ribosome	107	6,39	-6,48	GO:0004620	phospholipase activity	29	4,35	-2,41
GO:0010038	response to metal ion	85	6,15	-2,71	GO:0102483	scopolin beta-glucosidase activity	24	4,31	-0,41
GO:0048437	floral organ development	99	5,92	-2,11	GO:0010087	phloem or xylem histogenesis	63	4,25	-4,66
GO:0010646	regulation of cell communication	146	5,90	-5,96	GO:0007389	pattern specification process	112	4,23	-3,59
GO:0016829	lyase activity	114	5,84	-3,56	GO:0009826	unidimensional cell growth	148	4,20	-3,45
GO:0009733	response to auxin	140	5,77	-3,21	GO:0008283	cell population proliferation	44	4,07	-0,30
GO:0090693	plant organ senescence	120	5,68	-1,10	GO:0048438	floral whorl development	77	3,89	-1,03
GO:0010143	cutin biosynthetic process	18	5,06	-1,89	GO:1904680	peptide transmembrane transporter activity	21	3,83	-1,09
GO:0015267	channel activity	70	5,00	-2,15	GO:0030029	actin filament-based process	49	3,81	-3,00
GO:0009743	response to carbohydrate	70	4,90	-0,48	GO:0051923	sulfation	12	3,67	-2,31
GO:0006833	water transport	22	4,90	-2,13	GO:0009615	response to virus	40	3,63	-0,95
GO:0019900	kinase binding	51	4,87	-4,90	GO:0090351	seedling development	75	3,61	-1,27

GO:0005507	copper ion binding	68	4,66	-2,67	GO:0006972	hyperosmotic response	32	3,54	-0,71
GO:0070417	cellular response to cold	20	4,55	-1,79	GO:0006576	biogenic amine metabolic process	38	3,47	-3,57
GO:0006972	hyperosmotic response	33	4,45	-1,22	GO:0005509	calcium ion binding	85	3,36	-3,80
GO:0051094	positive regulation of developmental process	54	4,42	-2,18	GO:0009408	response to heat	122	3,23	-1,99
GO:0009723	response to ethylene	89	4,37	-2,23	GO:0030145	manganese ion binding	24	3,16	-2,45
GO:0051093	negative regulation of developmental process	67	4,33	-0,61	GO:0055086	nucleobase-containing small molecule metabolic process	124	3,10	-0,54
GO:0008171	O-methyltransferase activity	23	3,98	-1,04	GO:0009629	response to gravity	41	3,09	-1,72
GO:0005774	vacuolar membrane	69	3,92	-3,49	GO:0099503	secretory vesicle	60	3,03	-2,84
GO:1903338	regulation of cell wall organization or biogenesis	31	3,86	-4,49	GO:0009631	cold acclimation	25	2,94	-0,20
GO:0038023	signaling receptor activity	50	3,68	-1,13	GO:0006833	water transport	19	2,90	-2,06
GO:0035556	intracellular signal transduction	135	3,64	-3,87	GO:0035266	meristem growth	37	2,87	-0,16
GO:1901568	fatty acid derivative metabolic process	25	3,43	-1,40	GO:0016614	oxidoreductase activity acting on CH-OH group of donors	69	2,82	-0,12
GO:0090351	seedling development	71	3,43	-1,54	GO:0000981	DNA-binding transcription factor activity RNA polymerase II-specific	95	2,78	-0,31
GO:0050660	flavin adenine dinucleotide binding	55	3,34	-0,13	GO:0008171	O-methyltransferase activity	21	2,73	-1,09
GO:0008283	cell population proliferation	40	3,29	-2,21	GO:0044273	sulfur compound catabolic process	13	2,73	-2,50
GO:0006576	biogenic amine metabolic process	36	3,28	-4,00	GO:0005507	copper ion binding	63	2,68	-3,15
GO:0009826	unidimensional cell growth	135	3,14	-5,25	GO:1901698	response to nitrogen compound	84	2,64	-0,87
GO:0051923	sulfation	11	3,13	-2,71	GO:0009838	abscission	19	2,59	-2,06
GO:0005509	calcium ion binding	80	3,10	-4,70	GO:0032504	multicellular organism reproduction	81	2,58	-2,11
GO:0010073	meristem maintenance	83	3,03	-2,52	GO:0008236	serine-type peptidase activity	59	2,47	-1,95

GO:0009739	response to gibberellin	46	3,00	-0,59	GO:0042886	amide transport	20	2,47	-0,89
GO:0050829	defense response to Gram-negative bacterium	13	2,94	-1,94	GO:0008378	galactosyltransferase activity	20	2,47	-2,24
GO:0009735	response to cytokinin	47	2,83	-2,19	GO:0005615	extracellular space	46	2,38	-1,77
GO:0000981	DNA-binding transcription factor activity RNA polymerase II-specific	91	2,81	-3,04	GO:0010223	secondary shoot formation	17	2,30	-1,21
GO:0042578	phosphoric ester hydrolase activity	109	2,81	-3,54	GO:0000278	mitotic cell cycle	85	2,16	-4,23
GO:0008236	serine-type peptidase activity	58	2,79	-2,63	GO:0016311	dephosphorylation	70	2,10	-2,63
GO:0008378	galactosyltransferase activity	20	2,72	-2,24	GO:1901607	alpha-amino acid biosynthetic process	56	2,08	-1,60
GO:0051253	negative regulation of RNA metabolic process	75	2,68	-0,81	GO:0019199	transmembrane receptor protein kinase activity	18	2,05	-0,47
GO:0032504	multicellular organism reproduction	78	2,68	-4,08	GO:0044087	regulation of cellular component biogenesis	47	2,04	-3,94
GO:0099503	secretory vesicle	56	2,63	-2,94	GO:0015851	nucleobase transport	13	2,01	-0,83
GO:0030029	actin filament-based process	43	2,62	-3,81	GO:0006644	phospholipid metabolic process	67	1,94	-1,83
GO:0051302	regulation of cell division	30	2,42	-1,10	GO:0003008	system process	11	1,87	-1,51
GO:0009411	response to UV	42	2,36	-1,54	GO:0032879	regulation of localization	47	1,68	-1,60
GO:0042886	amide transport	19	2,33	-2,52	GO:0045927	positive regulation of growth	17	1,51	-0,24
GO:0030145	manganese ion binding	21	2,27	-2,40	GO:0009555	pollen development	104	1,43	-2,16
GO:0000079	regulation of cyclin-dependent protein serine/threonine kinase activity	20	2,25	-1,79					
GO:0015294	solute:monoatomic cation symporter activity	17	2,24	-0,73					
GO:0043094	cellular metabolic compound salvage	29	2,20	-0,56					
GO:0043621	protein self-association	40	2,16	-0,63					
GO:0009631	cold acclimation	22	2,12	-1,28					
GO:0009408	response to heat	109	2,08	-1,25					
GO:0008970	phospholipase A1 activity	9	2,02	-3,00					
GO:0003008	system process	11	2,00	-1,51					
GO:0000278	mitotic cell cycle	80	1,96	-5,81					

GO:009 9080	supramolecular complex	113	1,87	-4,80					
GO:000 5615	extracellular space	42	1,87	-3,09					
GO:190 1607	alpha-amino acid biosynthetic process	52	1,77	-1,11					
GO:001 0214	seed coat development	20	1,44	-2,24					
GO:000 9606	tropism	49	1,32	-2,14					
GO:005 5086	nucleobase-containing small molecule metabolic process	105	1,31	-0,88					

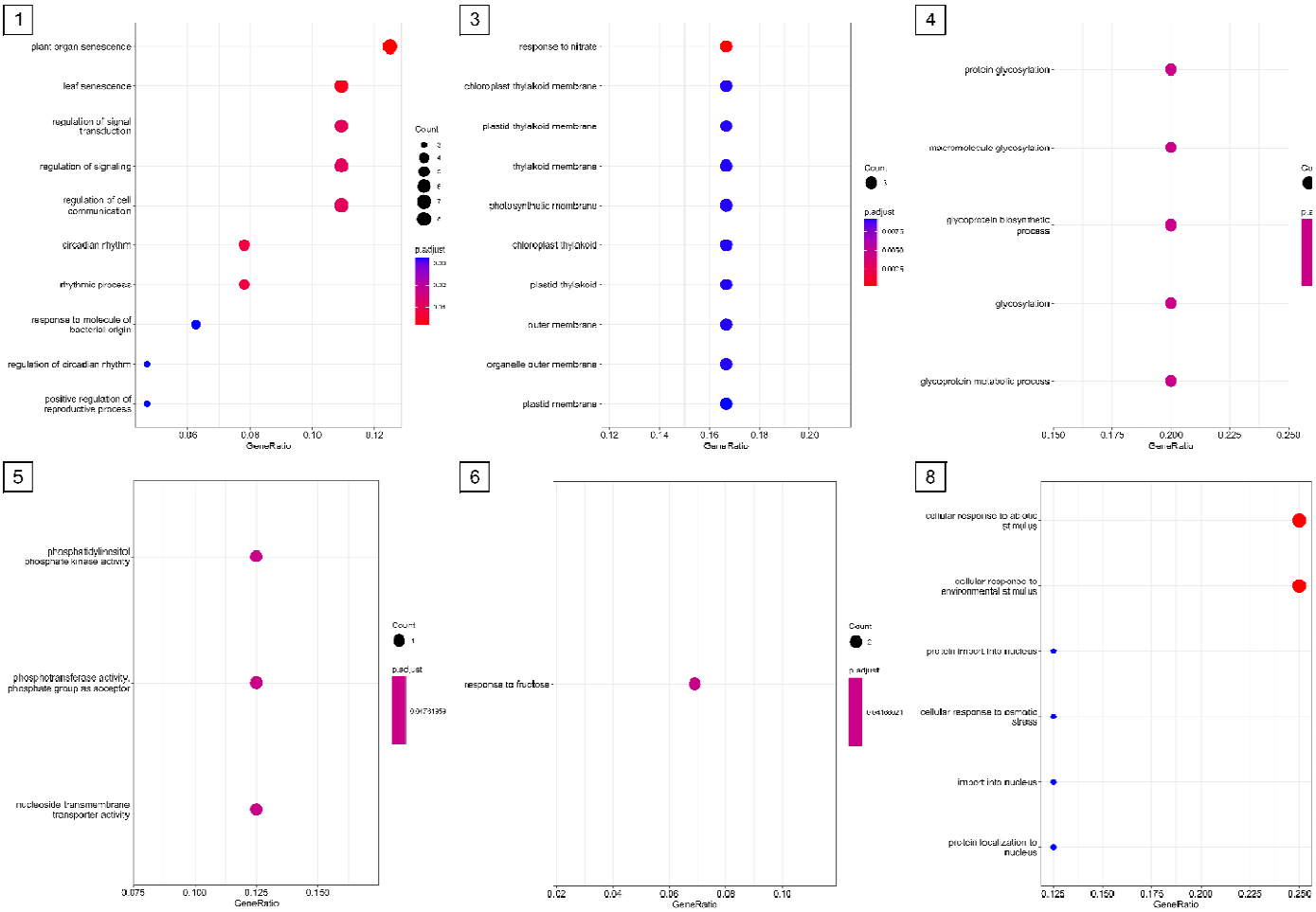

Additional File 8 GO terms overrepresentation analysis of clusters of DEGs driven by the interaction between infection and time of the day 14 DAI

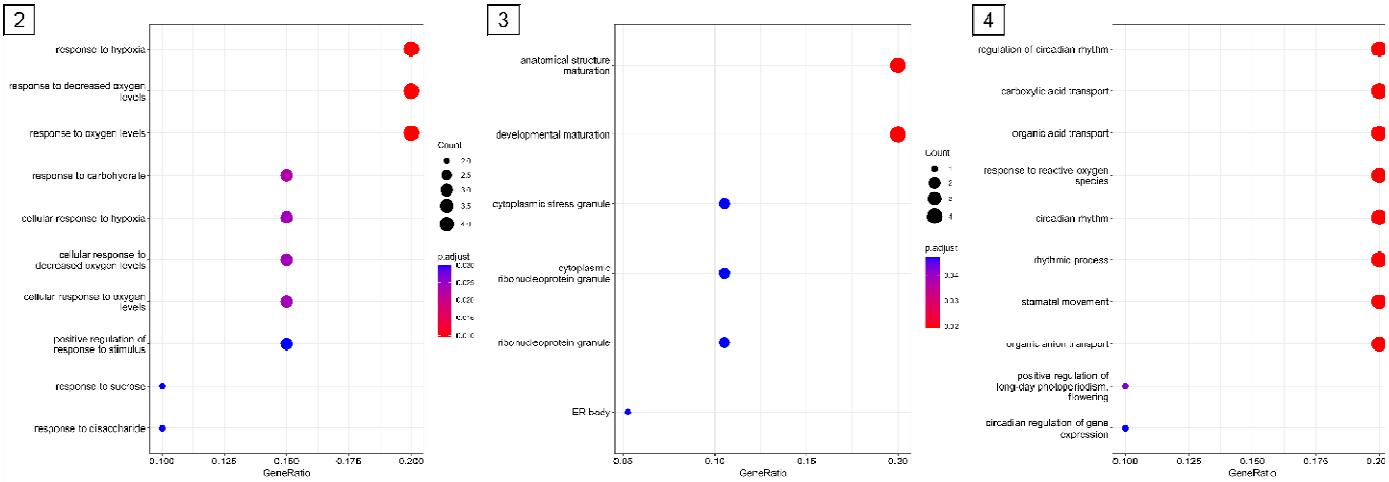

Additional File 9 GO terms overrepresentation analysis of clusters of DEGs driven by the interaction between infection and time of the day 21 DAI

https://fileshare.uibk.ac.at/f/03d6ddfe1e6145bca1a6/?dl=1

Additional File 10 Enriched GO terms and corresponding genes underpinning figure 2 and 3 before data reduction.